



# Hyaluronic acid-based pH-sensitive polymer-modified liposomes for cell-specific intracellular drug delivery systems

メタデータ	言語: eng 出版者: 公開日: 2019-01-25 キーワード (Ja): キーワード (En): 作成者: Miyazaki, Maiko, Yuba, Eiji, Hayashi, Hiroshi, Harada, Atsushi, Kono, Kenji メールアドレス: 所属:
URL	<a href="http://hdl.handle.net/10466/16172">http://hdl.handle.net/10466/16172</a>

1 **Hyaluronic acid-based pH-sensitive polymer-modified liposomes for cell-specific**  
2 **intracellular drug delivery systems**

3

4 Maiko Miyazaki<sup>1</sup>, Eiji Yuba<sup>1,\*</sup>, Hiroshi Hayashi<sup>2</sup>, Atsushi Harada<sup>1</sup>, and Kenji Kono<sup>1</sup>

5

6 <sup>1</sup>Department of Applied Chemistry, Graduate School of Engineering, Osaka Prefecture

7 University, 1-1 Gakuen-cho, Naka-ku, Sakai, Osaka 599-8531, Japan

8 <sup>2</sup>Science Lin Co., Ltd., 1-1-35 Nishiawaji, Higashiyodogawa-Ku, Osaka, Osaka 533-

9 0031, Japan

10

11 **\*Corresponding authors: Eiji Yuba**

12 Department of Applied Chemistry, Graduate School of Engineering,

13 Osaka Prefecture University, 1-1 Gakuen-cho, Naka-ku, Sakai, Osaka 599-8531, Japan

14 Tel: +81-722-54-9913; Fax: +81-722-54-9330; yuba@chem.osakafu-u.ac.jp

15 **Abstract**

16 For the enhancement of therapeutic effects and reduction of side effects derived from  
17 anticancer drugs in cancer chemotherapy, it is imperative to develop drug delivery  
18 systems with cancer-specificity and controlled release function inside cancer cells. pH-  
19 Sensitive liposomes are useful as an intracellular drug delivery system because of their  
20 abilities to transfer their contents into the cell interior through fusion or destabilization  
21 of endosome, which has weakly acidic environment. We earlier reported liposomes  
22 modified with various types of pH-sensitive polymers based on synthetic polymers and  
23 biopolymers as vehicles for intracellular drug delivery systems. In this study, hyaluronic  
24 acid (HA)-based pH-sensitive polymers were designed as multi-functional polymers  
25 having not only pH-sensitivity but also targeting properties to cells expressing CD44,  
26 which is known as a cancer cell surface marker. Carboxyl group-introduced HA  
27 derivatives of two types, MGlu-HA and CHex-HA, which have a more hydrophobic  
28 side chain structure than that of MGlu-HA, were synthesized by reaction with various  
29 dicarboxylic anhydrides. These polymer-modified liposomes were stable at neutral pH,  
30 but showed content release under weakly acidic conditions. CHex-HA-modified  
31 liposomes delivered their contents into CD44-expressing cells more efficiently than  
32 HA-modified or MGlu-HA-modified liposomes or unmodified liposomes, whereas the

33 same liposomes were taken up only slightly by cells expressing CD44 proteins less.  
34 Competition assay using free HA or other polymers revealed that HA derivative-  
35 modified liposomes might be recognized by CD44. Therefore, HA-derivative-modified  
36 liposomes are useful as cell-specific intracellular drug delivery systems.

37

38 *Keywords:* hyaluronic acid / pH-sensitive liposome / CD44 / drug delivery system /  
39 endosome / cancer chemotherapy

## 40 **Introduction**

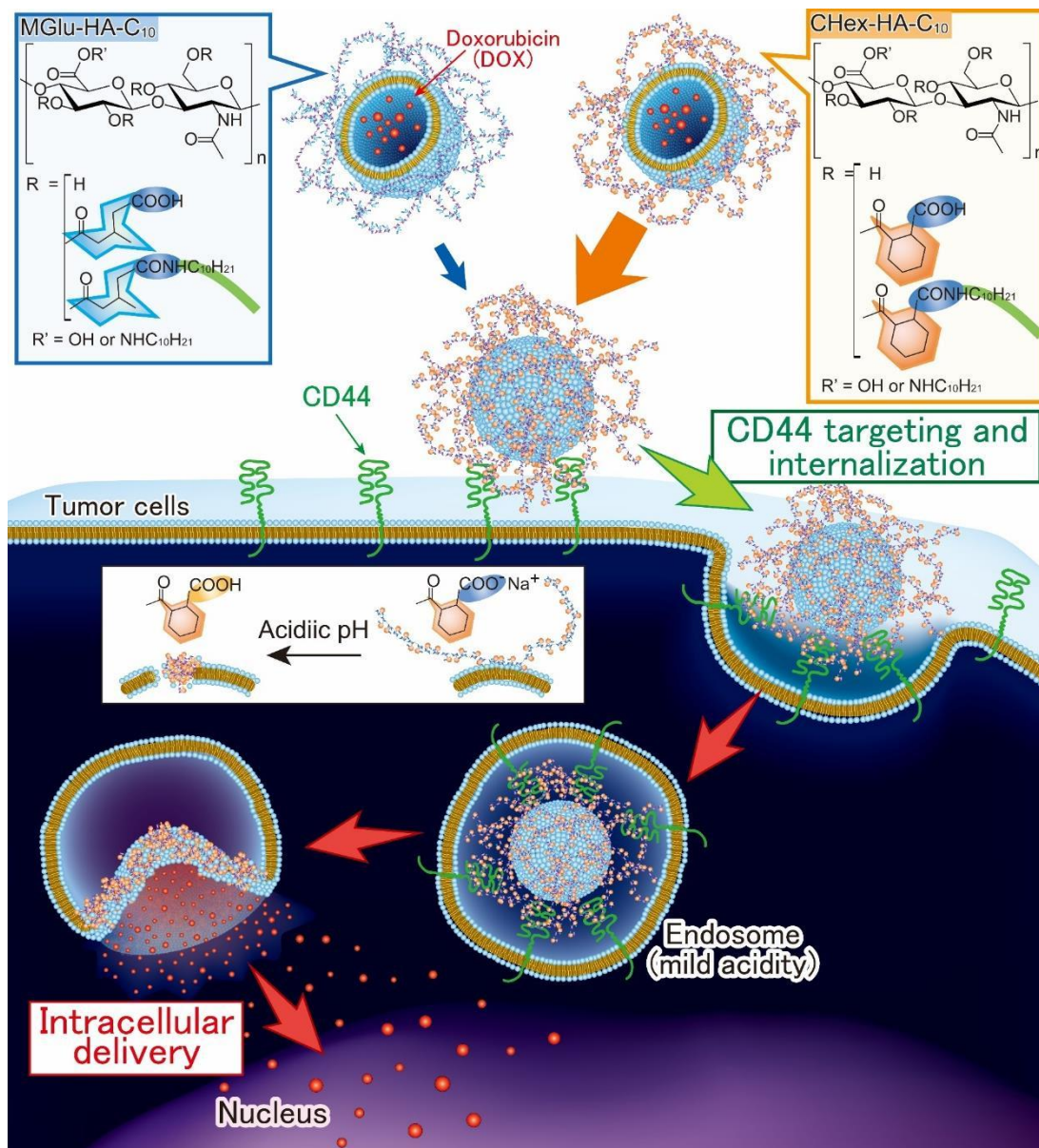
41 Cell-specific drug delivery is crucially important to develop highly effective  
42 therapeutic systems with less-adverse effects. Furthermore, most bio-pharmaceuticals  
43 should be delivered to target cell interior and to target organelles to express their drug  
44 efficacy. For this purpose, drug-loaded nanocarriers composed of polymeric materials or  
45 lipid-based materials have been studied intensively.<sup>1-3</sup> For cancer treatment, nano-sized  
46 drug carriers present benefits of reducing the spread of anticancer drugs to normal  
47 tissues or normal cells and of accumulating into tumor tissues via enhanced permeation  
48 and retention (EPR) effects.<sup>4</sup> For example, polymeric micelle-based systems having  
49 various sizes efficiently accumulated to tumor tissues. Furthermore, smaller polymeric  
50 micelles penetrated into tumor tissues more effectively.<sup>5</sup> Poly(ethylene glycol) (PEG)-  
51 modified liposome encapsulating doxorubicin (DOX), Doxil, is an example of a  
52 commercially available lipid-based nanocarrier that can achieve DOX delivery into  
53 tumor tissues via the EPR effect.<sup>6</sup> However, such a “passive targeting” approach  
54 requires more precise delivery of drugs directly to target cells only, in addition to  
55 control of drug release.<sup>2,7</sup> The insertion of ligand molecules having specificity to tumor-  
56 specific surface receptors or endothelial cells directly into neovascular vessels of a  
57 tumor is regarded as effective approach providing cancer cell specificity to

58 nanocarriers.<sup>8-11</sup> To control drug release profiles, external stimuli-sensitive properties  
59 such as temperature, pH, magnetic field and light have been applied for nanocarriers.<sup>12-</sup>  
60 <sup>21</sup> ThermoDox is one example of a temperature-responsive liposome designed to  
61 achieve drug release at tumor tissues under local heating of tumor tissues.<sup>22-24</sup>  
62 Temperature-sensitive polymer-modified liposomes are another platform to develop  
63 temperature-responsive liposomes.<sup>11,13</sup> The use of functional polymers might be  
64 beneficial to control temperature-sensitivity and temperature-regions to release  
65 anticancer drugs by changing polymer chemical structures. To obtain stimulus-  
66 responsive nanocarriers, pH is also an important external stimulus because tumor tissues  
67 possess lower pH than physiological pH. Moreover, weakly acidic pH intracellular  
68 compartments (endo/lysosomes) exist inside of cells. To deliver drugs or  
69 macromolecules into cytosol of target cells, pH-responsive liposomes have been  
70 developed. Mixtures of dioleoylphosphatidylethanolamine and amphiphiles having  
71 carboxyl groups act as pH-responsive liposomes because, at neutral pH, this mixture  
72 forms a bilayer structure by hydration derived from carboxyl groups, whereas a rapid  
73 transition to hexagonal II phase is generated after protonation of carboxyl groups,  
74 leading to membrane fusion or drug release.<sup>25</sup> Modification of polymers having  
75 carboxyl groups to liposomes is another strategy to obtain pH-responsive liposomes.

76 Poly(acrylic acid) derivative-modified liposomes show vigorous membrane disruptive  
77 activity under acidic pH because polymers become hydrophobic after protonation of  
78 carboxyl groups. The polymers interact with a lipid membrane via hydrogen bond  
79 formation with phosphate groups and hydrophobic interactions.<sup>26,27</sup> Furthermore, the pH  
80 region can be controlled by changing the hydrophobicity of poly(acrylic acid)  
81 derivatives, which changes the pKa of carboxyl groups.<sup>27</sup> We also prepared  
82 carboxylated poly(glycidol)s as a pH-responsive polymer for pH-sensitization of  
83 liposomes.<sup>28-30</sup> pKa and pH-sensitivity of carboxylated poly(glycidol)s were controlled  
84 by spacer units next to carboxyl groups: poly(glycidol) derivatives having more  
85 hydrophobic spacer structures exhibited higher pKa and stronger membrane disruptive  
86 properties.<sup>29</sup> We further introduced these pH-sensitive units to naturally occurring  
87 polysaccharides such as dextran, mannan, and curdlan.<sup>31-33</sup> Carboxylated  
88 polysaccharides also showed pH-responsive properties. These polysaccharide-modified  
89 liposomes delivered model proteins into cytosol of target cells effectively via membrane  
90 fusion with endosomes.<sup>31-33</sup> Polysaccharides are important as base materials because of  
91 their biodegradability and easy functionalization. In addition, the cell surface has many  
92 kinds of lectins, polysaccharide-specific receptors, which are useful for targeting ligands  
93 to specific cells.<sup>34-37</sup>

94           Considering this background, we conceived multifunctional polysaccharide  
95 derivatives having both specificity to tumor cells and pH-responsive properties for this  
96 study. Integration of DDS functionalities into one molecule or one nanocarrier is  
97 effective strategy to develop multifunctional DDS. Hyaluronic acid (HA) was selected  
98 as a backbone of the multifunctional pH-responsive polymer.<sup>38</sup> HA is a biocompatible  
99 material: it is a main component of the extracellular matrix. Moreover, also it is known  
100 to bind to CD44 proteins specifically as a surface receptor on cancerous cells.<sup>34,35,39-41</sup>  
101 However, in most cases, raw HA was used for just providing targeting properties to  
102 nanocarriers. Here, we extended our strategy for development of pH-responsive  
103 polymers to HA: 3-methyl glutarylated (MGlu) units or 2-carboxycyclohexane-1-  
104 carboxylated (CHex) units were introduced to HA, and their pH-responsive capabilities  
105 were assessed (Figure 1). Furthermore, cell-specific anticancer drug delivery using HA  
106 derivative-modified liposomes was examined.

107



108

109 **Figure 1.** Design of hyaluronic acid derivative-modified liposomes for CD44-  
 110 expressing cell-specific intracellular drug delivery. These liposomes are taken up by  
 111 cells *via* endocytosis and trapped in endosome. Its weakly acidic environment triggers  
 112 destabilization of the liposome, which induces release of drugs in endosome and their  
 113 transfer to cytosol *via* destabilization of endosome.

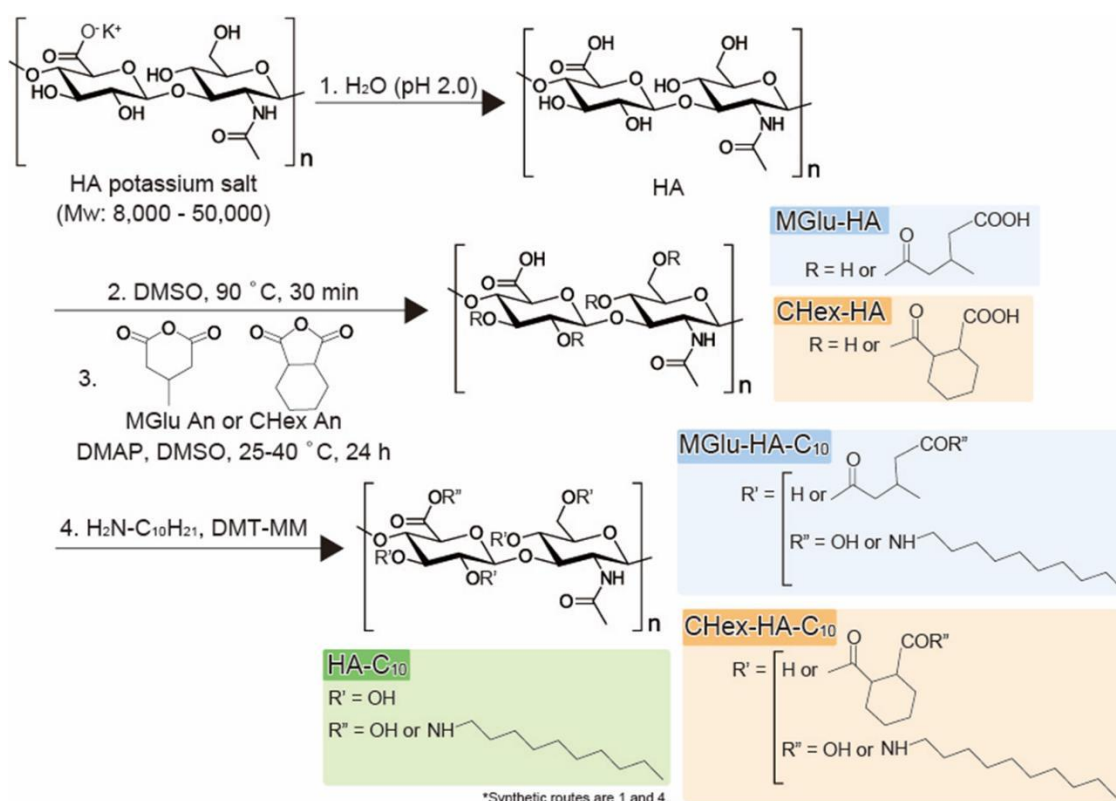
114

## 115 **Results and Discussion**

116 **Characterization of Hyaluronic Acid Derivatives.** Hyaluronic acid  
117 derivatives with different contents of MGlu groups or CHex groups as pH-sensitive  
118 moiety were synthesized by reacting HA with various amounts of 3-methylglutaric  
119 anhydride or 1,2-cyclohexanedicarboxylic anhydride (Figure 2 and Table 1). Decyl  
120 groups were further introduced to HA derivatives by reaction of decylamine with  
121 carboxyl groups in HA derivatives for fixation of these polymers onto liposome  
122 membrane (Figure 2 and Table 2). As a control, carboxyl groups of HA were reacted  
123 directly with decylamine to obtain anchor group-having HA (HA-C<sub>10</sub>). The obtained  
124 HA derivatives were characterized using <sup>1</sup>H NMR. Figures 3A–3C respectively  
125 represent <sup>1</sup>H NMR spectra of HA, MGlu<sub>52</sub>-HA, and MGlu<sub>57</sub>-HA-C<sub>10</sub>. In comparison to  
126 spectra for HA (Figure 3A) and for MGlu<sub>52</sub>-HA (Figure 3B), the introduction of MGlu  
127 groups to HA was confirmed from the existence of new peaks corresponding to MGlu  
128 groups (0.9 ppm, 1.9–2.3 ppm except for acetyl group of HA (2 ppm)) in Figure 3B.  
129 From the integration ratio of peaks of MGlu residues to those of sugar backbone (2  
130 ppm, 3.3–4.8 ppm), 52% of hydroxyl groups of HA was estimated as combined with  
131 MGlu residues. Similarly, from the integration ratio between sugar backbone, MGlu

132 residues, and decyl groups (0.9–1.4 ppm), decyl-amidated MGlu residues and MGlu  
 133 residues were found to be combined to 2% and 57% of hydroxyl groups of HA,  
 134 respectively, in the product, which is designated as MGlu<sub>57</sub>-HA-C<sub>10</sub>. CHex-HA  
 135 derivatives were also evaluated using the same procedure (Figures 3D and 3E). The  
 136 synthesis of HA-C<sub>10</sub> was also confirmed by the presence of decyl-amidated moieties  
 137 (0.9–1.4 ppm, Figure 3F). Compositions of HA derivatives prepared in this study are  
 138 presented in Tables 1 and 2.

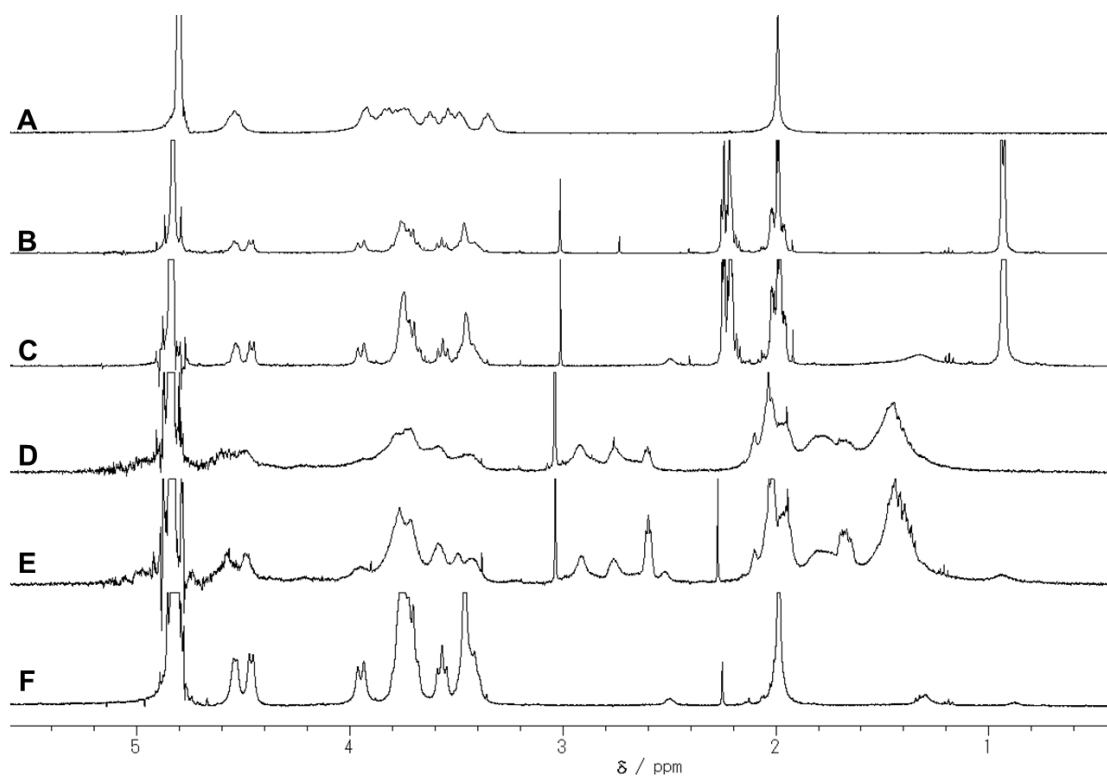
139



140

141 **Figure 2.** Synthetic route for hyaluronic acid derivatives having carboxyl groups and

142 alkyl chains as anchor units to liposomal membrane.



144

145 **Figure 3.**  $^1\text{H}$  NMR spectra of (A) hyaluronic acid, (B) MGlu<sub>52</sub>-HA, (C) MGlu<sub>57</sub>-HA-146 C<sub>10</sub>, (D) CHex<sub>60</sub>-HA, (E) CHex<sub>50</sub>-HA-C<sub>10</sub>, and (F) HA-C<sub>10</sub> in D<sub>2</sub>O/NaOD.

147

148

**Table 1. Synthesis of Hyaluronic Acid Derivatives**

Polymer	HA (mg)	DMAP (mg)	Dicarboxylic acid anhydride (mg)	DMSO (mL)	Reaction temperature (°C)	Yield (mg)	Yield (%)	MGlu or CHex (%)*
MGlu <sub>11</sub> -HA	266.2	161.8	286.5	25	25	201.4	73.4	11
MGlu <sub>18</sub> -HA	250.1	161.1	254.4	25	25	272.6	87.5	18
MGlu <sub>43</sub> -HA	104.8	66.1	210.7	10	40	144.2	120.2	43
MGlu <sub>52</sub> -HA	509.8	327.1	4852.9	50	40	647.8	87	52
CHex <sub>18</sub> -HA	1022.6	658.3	333.9	100	40	891.4	81.2	18
CHex <sub>27</sub> -HA	307.2	197.4	103.3	30	40	377.2	85.3	34
CHex <sub>34</sub> -HA	305.3	196.6	153.2	30	40	393.7	83	34

CHex<sub>60</sub>-HA 310 194.9 261 30 40 490.7 80 60

\*% for OH groups of HA determined by <sup>1</sup>H NMR.

149

150 **Table 2. Synthesis of Hyaluronic Acid Derivatives Having Anchor Moieties**

Polymer	MGlu-HA, CHex- HA or HA (mg)	n- Decylamine (mg)	DMT-MM (mg)	Water (mL)	Reaction time (h)	Yield (mg)	Yield (%)	Conversion (%)*	
								MGlu or CHex	C <sub>10</sub>
MGlu <sub>20</sub> -HA-C <sub>10</sub>	206.6	24.9	42.3	12	17	210	95.5	20	4
MGlu <sub>57</sub> -HA-C <sub>10</sub>	524.9	42.9	73.4	26	10	510	91.3	57	2
CHex <sub>27</sub> -HA-C <sub>10</sub>	302.4	33.5	65.5	18	23	270.9	84.4	27	6
CHex <sub>50</sub> -HA-C <sub>10</sub>	304.8	25.1	47.6	18	23	316.7	108.6	50	5
HA-C <sub>10</sub>	268.4	11.3	21.3	13	23	251.3	93.2	0	3

\*% for OH groups of HA determined by <sup>1</sup>H NMR.

151

152 Acid–base titration was conducted to assess the protonation behaviors of

153 carboxyl groups on HA derivatives (Figure 4). MGlu-HA and CHex-HA changed their

154 protonation state in the range of pH 4–10. Considering that p*K*<sub>a</sub> of carboxyl groups in

155 the parent HA is reported as 3.04 and that the protonation degree of these carboxyl

156 groups is less than 0.1 at pH 4.5,<sup>42</sup> the carboxyl groups in MGlu unit or CHex unit

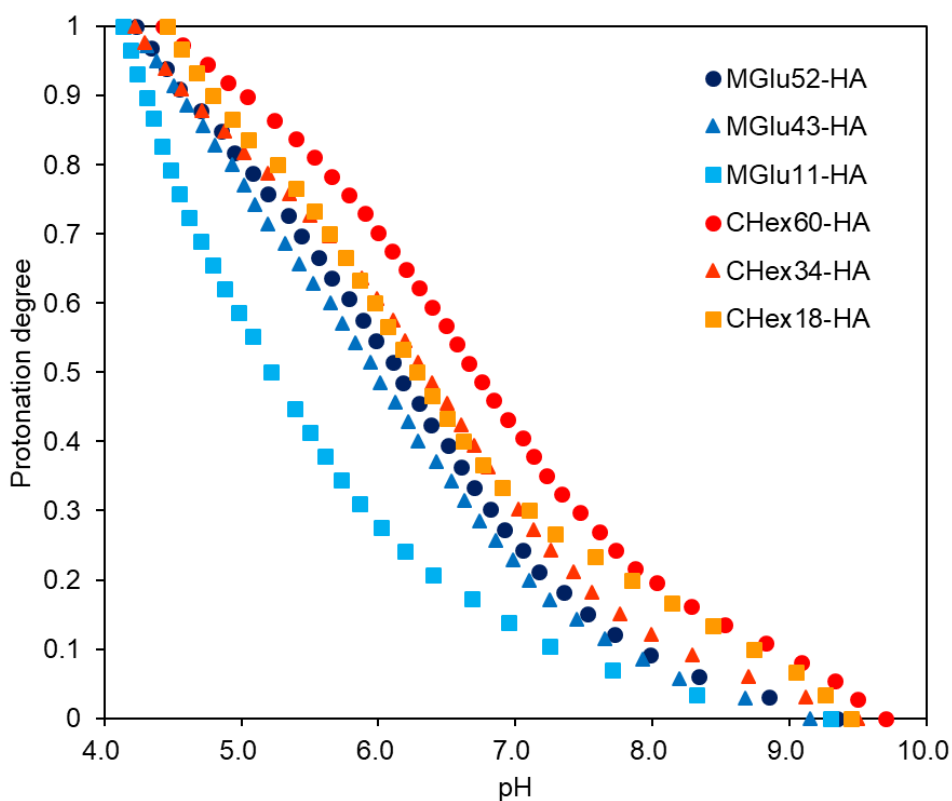
157 mainly changed their protonation state in the range of pH 4–10. The protonation

158 behaviors of HA derivatives were affected strongly by MGlu/CHex contents or a spacer

159 unit structure next to carboxyl groups. p*K*<sub>a</sub> of MGlu-HA/CHex-HA increased

160 concomitantly with increasing MGlu/CHex unit contents in HA derivatives (Table S1).

161 This result might derive from the promotion of protonation by a proximity effect of  
162 carboxyl groups, as described in our previous reports about poly(glycidol) derivatives or  
163 dextran derivatives.<sup>29,31,33</sup> In addition, CHex-HA showed higher  $pK_a$  value than that of  
164 MGlu-HA having the same amount of carboxylated units (Table S1), indicating that the  
165 more hydrophobic structure of CHex unit might promote the protonation of carboxyl  
166 groups more than the MGlu unit did. These HA derivatives had  $pK_a$  5.4–6.7 (Table S1),  
167 which corresponds to pH of early/late endosomes. Therefore, HA derivatives are  
168 expected to change their protonation state in these intracellular acidic compartments.  
169



170

**Figure 4.** Acid-base titration curves for HA derivatives.

171

172

173

To elucidate the pH-sensitivity of HA derivatives, we evaluated the interaction

174

of HA derivatives with a liposomal membrane. First, HA derivatives were added to

175

pyranine-loaded egg yolk phosphatidylcholine (EYPC) liposomes at various pH. Then,

176

the release of pyranine was monitored (Figure 5). Addition of HA-C<sub>10</sub> to liposome

177

affected the pyranine leakage from liposomes at any pH only slightly, which indicates

178

that the interaction of HA-C<sub>10</sub> with liposomal membrane might be low, irrespective of

179

the environmental pH. In contrast, addition of MGlu<sub>20</sub>-HA-C<sub>10</sub> and CHex<sub>27</sub>-HA-C<sub>10</sub>

180

suppressed the pyranine leakage at neutral pH compared with untreated liposomes

181

(Figures 5A and 5B), but gradually induced content release with decreasing pH (Figures

182

5C-E). These results suggest that the attachment of these polymers stabilized the

183

liposomal membrane but that the liposome membrane was destabilized gradually after

184

protonation of carboxyl groups in HA derivatives. However, the release percentage was

185

almost identical to that in the case of untreated liposomes, even after carboxyl groups

186

were protonated completely at pH 4 (Figure 4). For MGlu<sub>20</sub>-HA-C<sub>10</sub> and CHex<sub>27</sub>-HA-

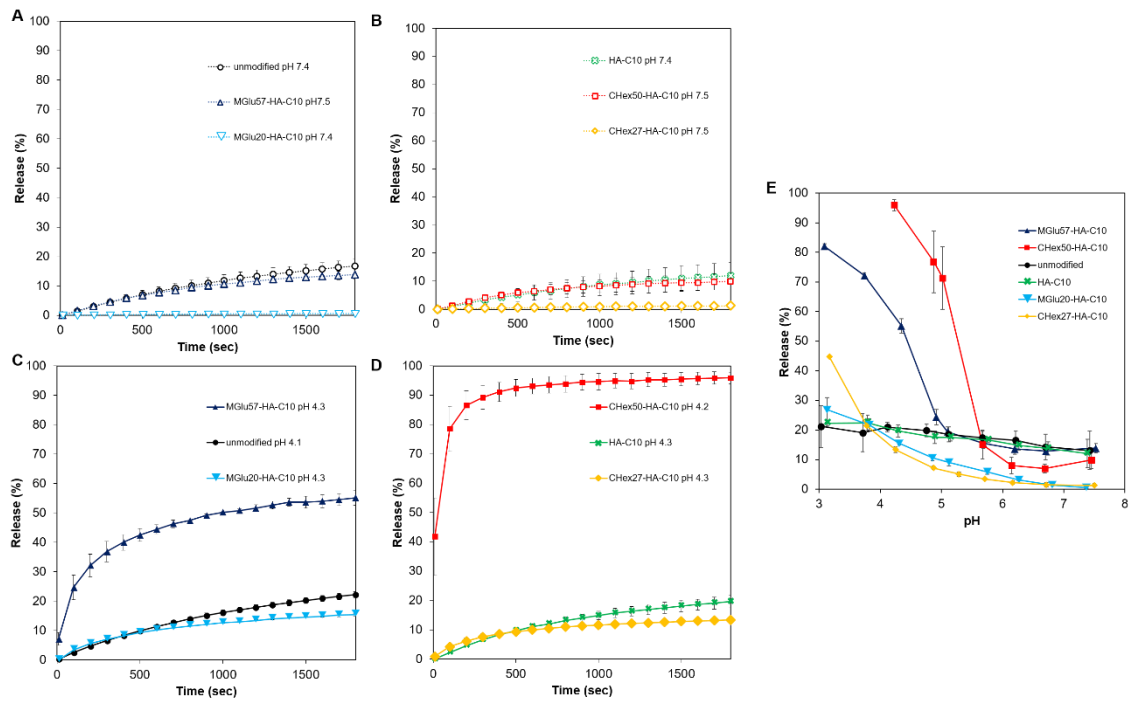
187

C<sub>10</sub>, the MGlu or CHex unit contents might be insufficient to destabilize the liposomal

188

membrane fully via hydrophobic interactions. MGlu<sub>57</sub>-HA-C<sub>10</sub> and CHex<sub>50</sub>-HA-C<sub>10</sub> also

189 only slightly affected the pyranine release at neutral pH (Figures 5A and 5B), but they  
190 exhibited significant content release at acidic pH within 5 min (Figures 5C and 5D).  
191 Considering the protonation curves of HA derivatives (Figure 4), more than 80% of  
192 carboxyl groups might be protonated at pH 5.1 or 5.7, where significant content release  
193 was induced respectively by MGlu<sub>57</sub>-HA-C<sub>10</sub> or CHex<sub>50</sub>-HA-C<sub>10</sub> (Figure 5E). After  
194 protonation of most carboxyl groups, these polymers might become hydrophobic and  
195 destabilize liposomal membrane within a few minutes. Results show that side chain  
196 structures and their contents can control the interaction of HA derivatives with  
197 liposomes. MGlu<sub>20</sub>-HA-C<sub>10</sub> and CHex<sub>27</sub>-HA-C<sub>10</sub> had pK<sub>a</sub> values of 5.4-6.4 (Table S1)  
198 but could not induce content release, whereas MGlu<sub>57</sub>-HA-C<sub>10</sub> or CHex<sub>50</sub>-HA-C<sub>10</sub>,  
199 which have pK<sub>a</sub> values of 6.1-6.7 (Table S1), showed significant contents release.  
200 Relatively high pK<sub>a</sub> values and high MGlu/CHex contents might be required for  
201 efficient destabilization of liposomal membranes.



202

203 **Figure 5.** Time-dependence (A-D) and pH-dependence (E) of pyranine release from egg

204 yolk phosphatidylcholine liposomes induced by various HA derivatives. Percent release

205 at neutral pH (A, B) and acidic pH (C, D) and release of pyranine after 30 min-

206 incubation (E) were shown. Polymer and lipid concentrations were 0.1 mg/mL and 2.0 ×

207 10<sup>-5</sup> M, respectively. Each point is the mean ± SD (*n* = 3).

208

209 **Preparation of Hyaluronic Acid Derivative-Modified Liposomes.** HA

210 derivative-modified liposomes were prepared using film hydration with a mixed thin

211 film of EYPC and HA derivatives. The liposome suspension was extruded further

212 through a polycarbonate membrane with 100 nm pore size. The size and zeta potential

213 of liposomes were investigated (Table 3 and Figure S1). All liposomes had narrow size  
214 distribution and average sizes were 130–200 nm, which is a suitable size for cellular  
215 uptake. HA derivative-modified liposomes showed more negative zeta potentials than  
216 those of unmodified liposomes or HA-C<sub>10</sub>-modified liposomes, indicating the  
217 modification of carboxylated HA derivatives onto the liposome surface. Pyranine-  
218 loaded liposomes were used to evaluate pH-responsive content release for liposomes  
219 (Figure 6). As shown in Figures 6A and 6B, all liposomes retained their contents at  
220 neutral pH, whereas MGlu<sub>57</sub>-HA-C<sub>10</sub>-modified liposomes and CHex<sub>50</sub>-HA-C<sub>10</sub>-modified  
221 liposomes induced content release within 10 min at acidic pH (Figures 6C and 6D),  
222 similarly to the results depicted in Figure 5. Figure 6E represents the pH-dependence of  
223 pyranine release from liposomes. Liposomes modified with HA-C<sub>10</sub> or HA derivatives  
224 having low MGlu/CHex units showed only slight content release under experimental  
225 conditions. In contrast, liposomes modified with HA derivatives having high  
226 MGlu/CHex units showed remarkable content release. Especially, CHex<sub>50</sub>-HA-C<sub>10</sub>-  
227 modified liposomes induced content release at a higher-pH region than that of MGlu<sub>57</sub>-  
228 HA-C<sub>10</sub>-modified liposomes, probably because intracellular compartments have weakly  
229 acidic pH (endo/lysosome). Therefore, CHex<sub>50</sub>-HA-C<sub>10</sub>-modified liposome is expected  
230 to respond to intracellular pH after internalization to cells.

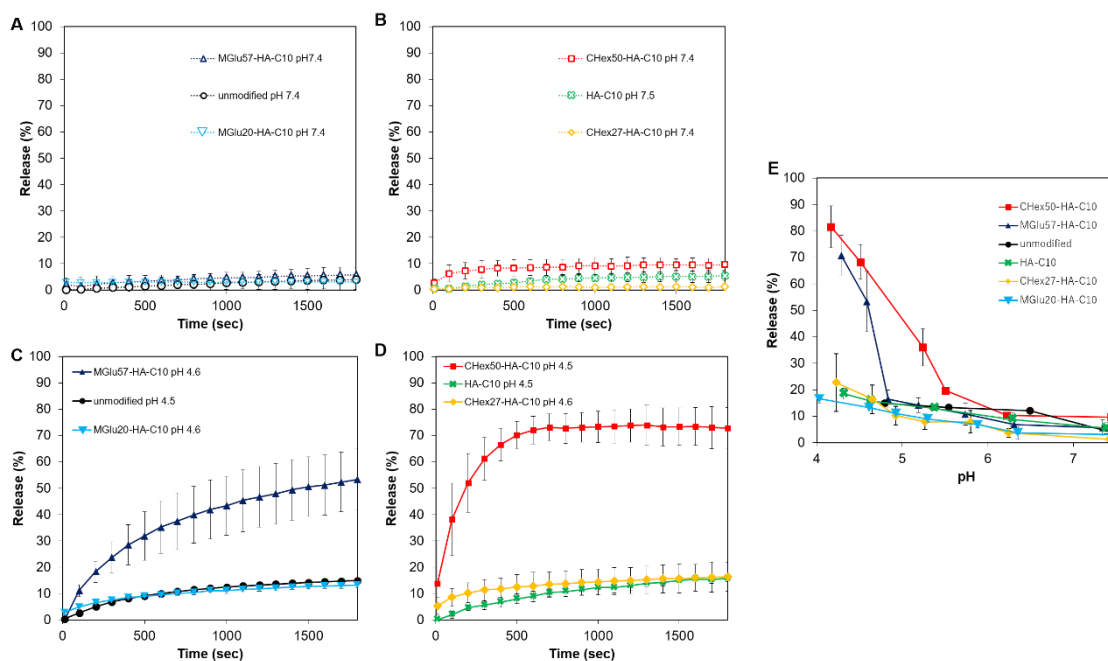
231

232

**Table 3. Particle Sizes and Zeta Potentials of Liposomes**

Liposome	Size (nm)	PdI	Zeta potential (mV)
Unmodified	193.5 ± 26.7	0.160 ± 0.107	-4.6 ± 0.3
HA-C <sub>10</sub>	160.9 ± 14.7	0.179 ± 0.071	-3.1 ± 0.3
MGlu <sub>20</sub> -HA-C <sub>10</sub>	191.5 ± 3.8	0.256 ± 0.030	-47.2 ± 0.4
MGlu <sub>57</sub> -HA-C <sub>10</sub>	144.8 ± 8.5	0.282 ± 0.007	-40.7 ± 2.1
CHex <sub>27</sub> -HA-C <sub>10</sub>	128.6 ± 6.1	0.133 ± 0.029	-46.7 ± 1.0
CHex <sub>50</sub> -HA-C <sub>10</sub>	140.8 ± 8.5	0.148 ± 0.019	-37.8 ± 1.9

233



234

235 **Figure 6.** pH-Sensitive contents release behaviors of HA derivative-modified

236 liposomes. Time courses at neutral pH (A, B) or at acidic pH (C, D) and pH-dependence

237 after 30 min-incubation (E) of pyranine release from liposomes modified with or

238 without HA derivatives were shown. Lipid concentrations were  $2.0 \times 10^{-5}$  M. Each

239 point is the mean  $\pm$  SD ( $n = 3$ ).

240

#### 241 **Interaction of Hyaluronic Acid Derivative-Modified Liposomes with Cells.**

242 Next, interaction of HA derivative-modified liposomes with cells was investigated.

243 CD44 protein on the cell surface might affect cellular association of HA derivative-

244 modified liposomes. Therefore, CD44 expression in various cells was evaluated using

245 fluorescence-labeled antibody for CD44. As shown in Figure S2, HeLa cells and

246 colon26 cells showed higher expression of CD44 than either MCF-7 cells or NIH3T3

247 cells. Considering these results, HeLa cells and colon26 cells were used respectively as

248 CD44<sup>high</sup> human-derived cells or mouse-derived cells, whereas MCF-7 cells and

249 NIH3T3 cells were used respectively as CD44<sup>low</sup> human-derived cells or mouse-derived

250 cell in the following experiments. After these cells were treated with DiI-labeled

251 liposomes modified with or without HA derivatives, their cellular fluorescence intensity

252 was ascertained using flow cytometric analysis. In the case of CD44<sup>high</sup> cells,

253 modification of HA-C<sub>10</sub> to EYPC liposomes increased the cellular association of

254 liposomes twice (Figures 7A and 7C), whereas cellular association of HA-C<sub>10</sub>-modified

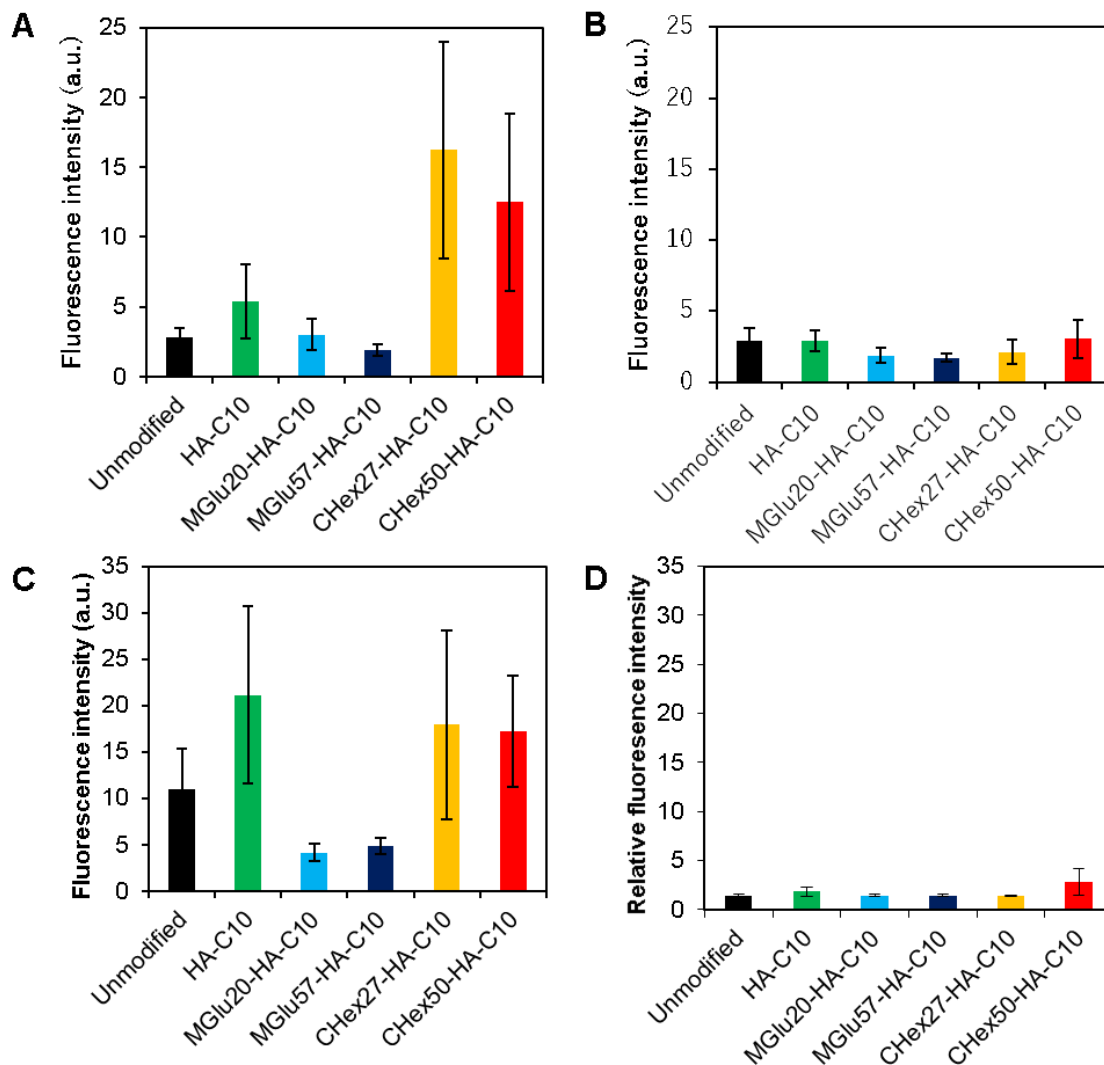
255 liposomes was identical to that of unmodified liposomes in the case of CD44<sup>low</sup> cells

256 (Figures 7B and 7D). These results indicate that HA on the liposome surface was

257 recognized by CD44 on HeLa cells or colon26 cells and that internalization of  
258 liposomes were promoted. MGlu-HA-C<sub>10</sub>-modified liposomes exhibited almost equal or  
259 less cellular association than that of unmodified liposomes, irrespective of the CD44  
260 expression on the cells (Figure 7). This equivalence suggests that introduction of MGlu  
261 groups to HA interferes with the interaction of HA derivatives with CD44 protein.  
262 Alternatively, the negative charge of MGlu-HA-C<sub>10</sub>-modified liposomes (Table 3)  
263 suppressed cellular association of liposomes. By contrast, CHex-HA-C<sub>10</sub>-modified  
264 liposomes showed much higher cellular uptake by CD44<sup>high</sup> cells alone than by  
265 unmodified liposomes (Figures 7A and 7C). Particularly, three-times-higher  
266 fluorescence intensity was observed from CHex-HA-C<sub>10</sub>-modified liposome-treated  
267 HeLa cells than from HA-C<sub>10</sub>-modified liposomes (Figure 7A). According to our earlier  
268 report, CHex unit-introduced dextran derivatives exhibited much higher cellular  
269 association than MGlu unit-introduced dextran because of its hydrophobic spacer  
270 structure.<sup>33</sup> However, in the case of HA derivatives, introduction of CHex units to HA  
271 showed enhanced cellular association to CD44<sup>high</sup> cells but no effect to CD44<sup>low</sup> cells  
272 (Figure 7). Hydrophobicity of CHex units might be suppressed by hydrophilic HA  
273 backbone compared with dextran. These results suggest that not hydrophobic interaction  
274 but interaction via CD44 contributes to the cellular association of CHex-HA-C<sub>10</sub>-

275 modified liposomes.

276



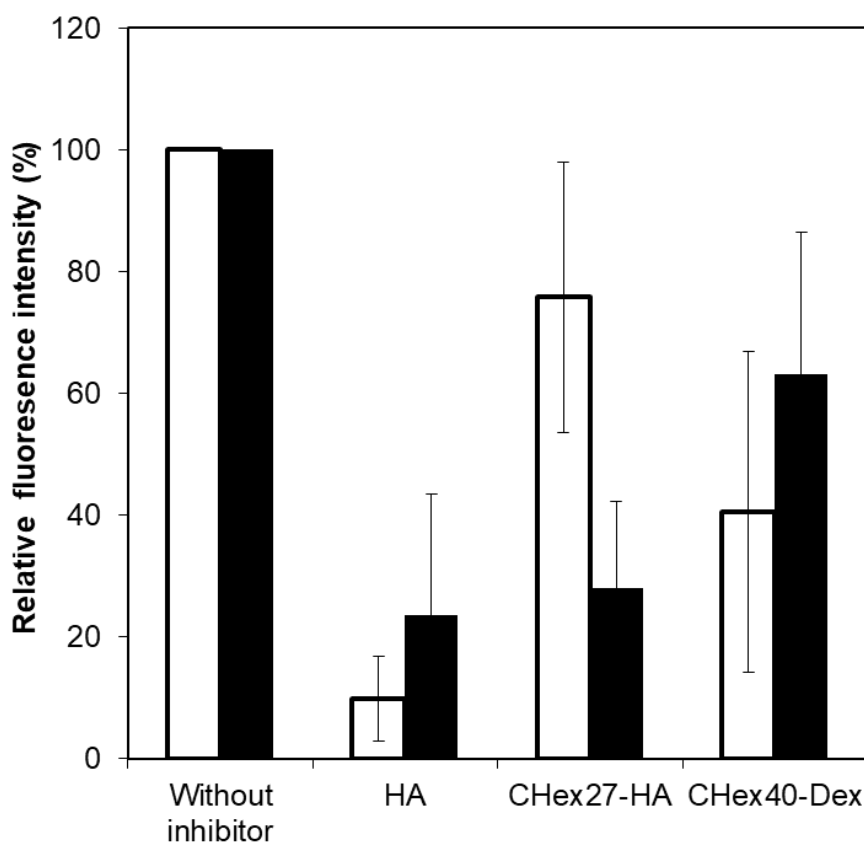
277 **Figure 7.** Fluorescence intensity for HeLa cells (A), MCF-7 cells (B), Colon26 cells  
278 (C), and NIH3T3 cells (D) treated with DiI-labeled EYPC liposomes modified with or  
279 without HA derivatives. Cells were incubated with liposomes (lipid concentration: 0.5  
280 mM) for 4 h at 37 °C in serum free medium. Cellular auto fluorescence was corrected.

281

282 To elucidate the uptake mechanism of HA derivative-modified liposomes,  
283 competition assay was applied (Figure 8). HeLa cells were treated with HA-C<sub>10</sub>-  
284 modified liposomes or CHex<sub>27</sub>-HA-C<sub>10</sub>-modified liposome in the presence of various  
285 inhibitors. Cellular association of HA-C<sub>10</sub>-modified liposomes was suppressed strongly  
286 in the presence of free HA, which indicates that HA-C<sub>10</sub>-modified liposomes were  
287 surely taken up via CD44 on HeLa cells. Cellular association of CHex<sub>27</sub>-HA-C<sub>10</sub>-  
288 modified liposomes was also suppressed by free HA, indicating that these liposomes  
289 were also recognized by CD44 and that introduction of CHex units did not interfere  
290 with the interaction with CD44. For the case in which that CHex<sub>27</sub>-HA without decyl  
291 groups were used as an inhibitor, cellular association of HA-C<sub>10</sub>-modified liposomes  
292 decreased slightly but that of CHex<sub>27</sub>-HA-C<sub>10</sub>-modified liposome was reduced  
293 considerably. These results suggest that not only CD44 recognition but also CHex  
294 groups contribute to the cellular association of CHex<sub>27</sub>-HA-C<sub>10</sub>-modified liposomes. To  
295 evaluate the effects of CHex groups on cellular association, CHex group-introduced  
296 dextran (CHex<sub>40</sub>-Dex)<sup>33</sup> was used for comparison. Results show that CHex<sub>40</sub>-Dex did  
297 not affect the cellular association of CHex<sub>27</sub>-HA-C<sub>10</sub>-modified liposome to any great  
298 degree. The same tendency was obtained when using colon 26 cells (Figure S3).  
299 Therefore, both CHex group and HA backbone might be necessary to enhance the

300 cellular association of liposomes to CD44-expressing cells. CHex units might promote  
301 the binding of HA backbone to CD44 proteins via hydrophobic interaction or  
302 cyclohexyl structure itself, which is the same backbone structure with polysaccharides.  
303 These results suggest that the introduction of CHex groups to HA is effective for  
304 promoting liposome uptake by CD44-expressing cells.

305



306

307 **Figure 8.** Inhibition of cellular association of HA-C<sub>10</sub>-modified liposomes (open bars)  
308 and CHex<sub>27</sub>-HA-C<sub>10</sub>-modified liposomes (closed bars) by various inhibitors. HeLa cells  
309 were pre-incubated with various inhibitors for 1 h before liposome treatment. Relative

310 fluorescence intensity was calculated as the ratios of the amount of association in the  
311 presence of inhibitor to that in the absence of inhibitor.

312

313 **Intracellular Delivery of Anticancer Drugs by Hyaluronic Acid Derivative-**

314 **Modified Liposomes.** Finally, the intracellular distribution of liposomes was examined.

315 DiI-labeled liposomes were applied to HeLa cells. Then DiI fluorescence in the cells

316 were detected using confocal laser scanning microscopy (Figure 9). For cells treated

317 with unmodified liposomes and MGlu<sub>57</sub>-HA-C<sub>10</sub>-modified liposomes, most DiI

318 fluorescence was observed from the periphery of cells (Figures 9A and 9C). In the cases

319 of HA-C<sub>10</sub>-modified liposomes and CHex<sub>50</sub>-HA-C<sub>10</sub>-modified liposomes, DiI

320 fluorescence was found to exist not only at the cellular periphery but also inside of the

321 cells as punctate fluorescence (Figures 9B and 9D). These results indicate that the

322 recognition of HA-C<sub>10</sub>-modified liposomes and CHex<sub>50</sub>-HA-C<sub>10</sub>-modified liposomes by

323 CD44 better promote the internalization of liposomes than the recognition of other

324 liposomes. Intracellular distribution of liposomes were further analyzed by staining of

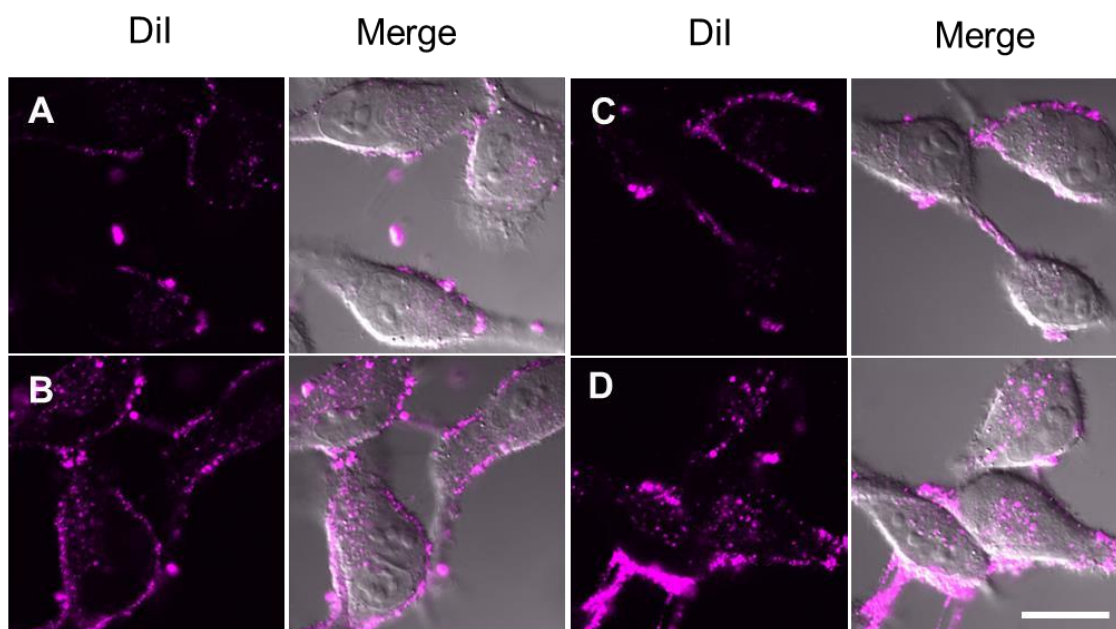
325 intracellular acidic compartments (endosomes and lysosomes) (Figure S4). Liposome-

326 derived fluorescence dots inside of cells were overlapped with fluorescence derived

327 from LysoTracker, which indicates that liposomes were trapped in endosome or

328 lysosomes after internalization to the cells.

329



330

331 **Figure 9.** Confocal laser scanning microscopic (CLSM) images of HeLa cells treated

332 with DiI-labeled EYPC liposomes modified without (A) or with HA-C<sub>10</sub> (B), MGLu<sub>57</sub>-

333 HA-C<sub>10</sub> (C) and CHex<sub>50</sub>-HA-C<sub>10</sub> (D) for 4 h at 37 °C in serum-free medium. Bar

334 represents 20 μm.

335

336 Intracellular drug delivery performance was investigated further. An anticancer

337 drug (DOX) was encapsulated to liposomes using remote loading method.<sup>43</sup> The

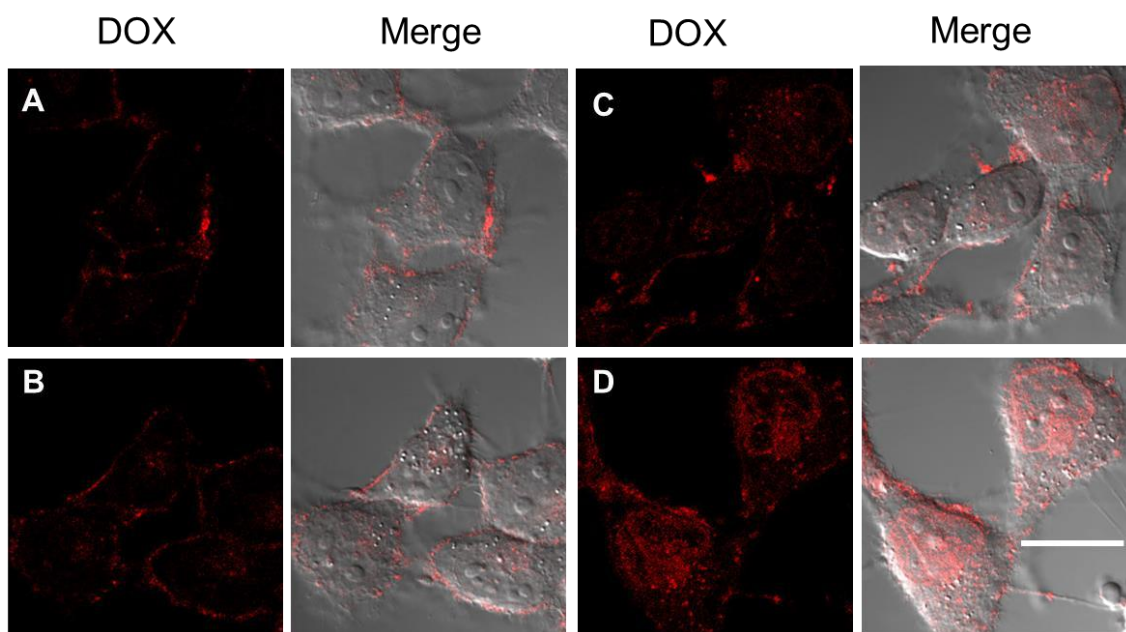
338 encapsulation efficiency of DOX was higher than 95% for unmodified liposomes and

339 HA-C<sub>10</sub>-modified liposomes, but 70–80% for MGLu<sub>57</sub>-HA-C<sub>10</sub>-modified liposomes and

340 CHex<sub>50</sub>-HA-C<sub>10</sub>-modified liposomes (Table S2). This result might derive from slight  
341 destabilization of liposomal membrane during the preparation of MGlu<sub>57</sub>-HA-C<sub>10</sub>- or  
342 CHex<sub>50</sub>-HA-C<sub>10</sub>-modified liposomes because the lipid membrane was dispersed in pH  
343 6.0 aqueous solution for preparing pH gradient to encapsulate DOX. However, these  
344 liposomes retained nanometer size and negative zeta potentials after DOX loading  
345 (Figure S5 and Table S2). HeLa cells were incubated with DOX-loaded liposomes.  
346 Then the intracellular distribution of DOX was detected using CLSM (Figure 10). For  
347 cells treated with unmodified liposomes, DOX fluorescence was observed from the cell  
348 periphery as with Figure 9 (Figure 10A). In the case of HA-C<sub>10</sub>-modified liposome-  
349 treated cells, dotted DOX fluorescence was observed from the periphery and inside of  
350 the cells (Figure 10B). This observation suggests that HA-C<sub>10</sub>-modified liposomes were  
351 taken up by cells, but they were trapped in endo/lysosomes because of their pH-  
352 insensitive properties. By contrast, cells treated with HA derivative-modified liposomes  
353 showed punctate fluorescence within cells and diffused fluorescence in the nucleus  
354 (Figures 10C and 10D). Particularly, CHex<sub>50</sub>-HA-C<sub>10</sub>-modified liposomes exhibited  
355 high performance to deliver DOX into the nucleus. These results reflect the pH-  
356 responsive membrane disruptive ability (Figures 5 and 6) and high cellular association  
357 (Figure 7) of HA derivatives. Results show that HA-derivative-modified liposomes

358 were internalized to cells and were trapped in endo/lysosomes (Figure S4).  
359 Subsequently, HA derivatives might become hydrophobic responding to acidic pH in  
360 endo/lysosomes and might destabilize liposomes and endo/lysosomal membrane,  
361 leading to delivery of DOX into cytosol and accumulation of DOX into the nucleus,  
362 whereas DiI fluorescence was observed from the same location with endo/lysosomes  
363 because of its hydrophobic property (Figure S4). Compared with MGlu<sub>57</sub>-HA-C<sub>10</sub>-  
364 modified liposomes, CHex<sub>50</sub>-HA-C<sub>10</sub>-modified liposomes better induced content release  
365 in a high-pH region (Figure 6). Therefore, CHex<sub>50</sub>-HA-C<sub>10</sub>-modified liposomes might  
366 respond to pH decrease in endosomes with earlier timing and might show higher  
367 intracellular delivery performance than MGlu<sub>57</sub>-HA-C<sub>10</sub>-modified liposomes show.  
368 Consequently, liposomes modified with HA derivatives, particularly CHex group-  
369 introduced HA derivatives, might be effective as intracellular drug delivery carriers to  
370 CD44-expressing cancerous cells. To elucidate DDS performance of CHex group-  
371 introduced HA derivative-modified liposome, cytotoxicity against HeLa cells was  
372 investigated (Figure S6). Compared with DOX-loaded liposomes without HA  
373 derivatives, DOX-loaded CHex<sub>50</sub>-HA-C<sub>10</sub>-modified liposomes exhibited strong  
374 cytotoxicity, which is comparable with free DOX. These results reflect the efficient  
375 DOX delivery to nucleus by CHex<sub>50</sub>-HA-C<sub>10</sub>-modified liposomes (Figure 10D).

376



377

378 **Figure 10.** CLSM images of HeLa cells treated with DOX-loaded EYPC liposomes  
379 modified without (A) or with HA-C<sub>10</sub> (B), MGl<sub>u57</sub>-HA-C<sub>10</sub> (C) and CHex<sub>50</sub>-HA-C<sub>10</sub> (D)  
380 for 4 h at 37 °C in serum-free medium. Bar represents 20 μm.

381

### 382 **Conclusion**

383 For this study, hyaluronic acid derivatives having pH-sensitivity and targeting  
384 ability were developed. MGl<sub>u</sub> unit-introduced or CHex unit-introduced hyaluronic acid  
385 derivatives induced lipid membrane disruptive activity in response to acidic pH. CHex  
386 unit-introduced hyaluronic acid derivative-modified liposomes exhibited high cellular  
387 association to highly CD44-expressing cells, whereas the same liposomes were taken up

388 only to a slight degree by CD44-low cells. These liposomes can deliver anticancer drugs  
389 to the interior of cells via pH-responsive membrane disruptive ability in  
390 endo/lysosomes. Therefore, pH-sensitive hyaluronic acid derivative-modified liposomes  
391 are promising as CD44-positive cell-specific intracellular drug delivery systems.

392

393 **Materials and Methods**

394 **Materials.** Egg yolk phosphatidylcholine (EYPC) was kindly donated by NOF Co.  
395 (Tokyo, Japan). 3-Methylglutaric anhydride, 1,2-cyclohexanedicarboxylic anhydride  
396 and *p*-xylene-bis-pyridinium bromide (DPX) were purchased from Sigma (St. Louis,  
397 MO.). Hyaluronic acid potassium salt (Mw:8,000-50,000), 1-aminodecane, pyranine  
398 and Triton X-100 were obtained from Tokyo Chemical Industries Ltd. (Tokyo, Japan).  
399 4-Dimethylaminopyridine (DMAP) was obtained from nacalai tesque (Kyoto, Japan). 4-  
400 (4,6-Dimethoxy-1,3,5-triazin-2-yl)-4-methyl morpholinium chloride (DMT-MM) was  
401 from Wako Pure Chemical Industries Ltd. (Osaka, Japan). 1,1'-Dioctadecyl-3,3',3'-  
402 tetramethylindocarbocyanine perchlorate (DiI) was from Life technologies. pH-sensitive  
403 dextran derivative (CHex<sub>40</sub>-Dex) was prepared as previously reported.<sup>33</sup> Doxorubicin  
404 (DOX) was kindly donated by Kyowa Hakko Kirin Co. Ltd. (Tokyo, Japan).

405

406 **Synthesis of Hyaluronic Acid Derivatives.** Hyaluronic acid potassium salt was first  
407 converted to free acidic form by addition of hydrochloric acid (pH 2.0) and  
408 subsequently lyophilized. 3-Methyl-glutarylated hyaluronic acid (MGlu-HA) and 2-  
409 carboxycyclohexane-1-carboxylated hyaluronic acid (CHex-HA) were prepared by  
410 reaction of hyaluronic acid with 3-methylglutaric anhydride and 1,2-

411 cyclohexanedicarboxylic anhydride, respectively. A given amount of dimethyl sulfoxide  
412 (DMSO) was added to hyaluronic acid and stirred at 90 °C for 30 min under argon  
413 atmosphere. After cooling to room temperature, DMAP and dicarboxylic anhydrides  
414 were added to DMSO solution of HA. The mixed solution was kept at a given  
415 temperature for 24 h with stirring under argon atmosphere. Then, saturated sodium  
416 hydrogen carbonate aqueous solution was added to the reaction mixture for  
417 neutralization and the reaction mixture was dialyzed against water for 3 days. The  
418 product was recovered by freeze-drying. <sup>1</sup>H NMR for MGlu-HA (400 MHz,  
419 D<sub>2</sub>O+NaOD) : δ 0.9 (s, -CO-CH<sub>2</sub>-CH(CH<sub>3</sub>)-CH<sub>2</sub>-), 1.9 – 2.3 (br, -CO-CH<sub>2</sub>-CH(CH<sub>3</sub>)-  
420 CH<sub>2</sub>-, -NH-CO(CH<sub>3</sub>)), 3.3 – 4.0 (br, glucose 2H, 3H, 4H, 5H, 6H), 4.6-4.8 (br, glucose  
421 1H). <sup>1</sup>H NMR for CHex-HA (400 MHz, D<sub>2</sub>O+NaOD) : δ 1.3-2.2 (m, -cyclo-CH<sub>2</sub>, -NH-  
422 CO(CH<sub>3</sub>)), 2.6-3.0 (m, cyclo-CH), 3.3 – 4.0 (br, glucose 2H, 3H, 4H, 5H, 6H), 4.6 – 4.8  
423 (br, glucose 1H).

424 As anchor moieties for fixation of MGlu-HA, CHex-HA and HA onto  
425 liposome membranes, 1-aminodecane was combined with carboxyl groups of MGlu-  
426 HA, CHex-HA and HA. Each polymer was dissolved in water around pH 7.4, and 1-  
427 aminodecane (0.1 equiv. to hydroxyl group of polymer) was reacted to carboxyl groups  
428 of the polymer using DMT-MM (0.1 equiv. to hydroxyl group of polymer) at room

429 temperature for 10-23 h with stirring. The obtained polymers were purified by dialysis  
430 in water. The compositions for polymers were estimated using <sup>1</sup>H NMR. <sup>1</sup>H NMR for  
431 MGlu-HA-C<sub>10</sub> (400 MHz, D<sub>2</sub>O+NaOD) : δ 0.9 (s, -CO-CH<sub>2</sub>-CH(CH<sub>3</sub>)-CH<sub>2</sub>-, -CO-NH-  
432 CH<sub>2</sub>-(CH<sub>2</sub>)<sub>8</sub>-CH<sub>3</sub>), 1.2 – 1.4 (br, -CO-NH-CH<sub>2</sub>-(CH<sub>2</sub>)<sub>8</sub>-CH<sub>3</sub>), 1.9 – 2.3 (br, -CO-CH<sub>2</sub>-  
433 CH(CH<sub>3</sub>)-CH<sub>2</sub>-, -NH-CO(CH<sub>3</sub>)), 2.5 (br, -CO-NH-CH<sub>2</sub>-(CH<sub>2</sub>)<sub>8</sub>-CH<sub>3</sub>), 3.3 – 4.0 (br,  
434 glucose 2H, 3H, 4H, 5H, 6H), 4.6-4.8 (br, glucose 1H). <sup>1</sup>H NMR for CHex-HA-C<sub>10</sub>  
435 (400 MHz, D<sub>2</sub>O+NaOD) : δ 0.9 (br, -CO-NH-CH<sub>2</sub>-(CH<sub>2</sub>)<sub>8</sub>-CH<sub>3</sub>), 1.3-2.2 (m, -cyclo-  
436 CH<sub>2</sub>-, -CO-NH-CH<sub>2</sub>-(CH<sub>2</sub>)<sub>8</sub>-CH<sub>3</sub>-, -NH-CO(CH<sub>3</sub>)), 2.6-3.0 (m, cyclo-CH), 3.2 (br, -CO-  
437 NH-CH<sub>2</sub>-(CH<sub>2</sub>)<sub>8</sub>-CH<sub>3</sub>), 3.3 – 4.0 (br, glucose 2H, 3H, 4H, 5H, 6H), 4.6 – 4.8 (br,  
438 glucose 1H). <sup>1</sup>H NMR for HA-C<sub>10</sub> (400 MHz, D<sub>2</sub>O+NaOD) : δ 0.9 (br, -CO-NH-CH<sub>2</sub>-  
439 (CH<sub>2</sub>)<sub>8</sub>-CH<sub>3</sub>), 1.2-1.4 (m, -CO-NH-CH<sub>2</sub>-(CH<sub>2</sub>)<sub>8</sub>-CH<sub>3</sub>) 1.9-2.0 (s, -NH-CO(CH<sub>3</sub>)), 2.5  
440 (br, -CO-NH-CH<sub>2</sub>-(CH<sub>2</sub>)<sub>8</sub>-CH<sub>3</sub>), 3.3 – 4.0 (br, glucose 2H, 3H, 4H, 5H, 6H), 4.6 – 4.8  
441 (br, glucose 1H).

442

443 **Titration.** To 40 mL of an aqueous solution of each polymer (carboxylate  
444 concentration:  $3.0 \times 10^{-4}$  M) was added an appropriate amount of 0.1 M NaOH solution  
445 to make pH 11.0. The titration was carried out by the stepwise addition of 0.01 M HCl  
446 solution at 25 °C, and pH and conductivity of the solution were monitored.

447

448 **Cell Culture.** Human cervix adenocarcinoma-derived HeLa cell, human breast cancer-  
449 derived MCF-7 cell and murine embryo fibroblast-derived NIH3T3 cell were grown in  
450 DMEM supplemented with 10% FBS (MP Biomedical, Inc.) and antibiotics at 37 °C.  
451 Murine colon adenocarcinoma-derived Colon-26 cell was grown in RPMI-1640  
452 supplemented with 10% FBS and antibiotics at 37 °C.

453

454 **Preparation of Liposomes.** To a dry, thin membrane of EYPC (10 mg) was dispersed  
455 in aqueous 35 mM pyranine, 50 mM DPX, and 25 mM phosphate solution (pH 7.4, 1.0  
456 mL). The liposome suspension was further hydrated by freezing and thawing, and was  
457 extruded through a polycarbonate membrane with a pore size of 100 nm. The liposome  
458 suspension was purified with ultracentrifugation for 2 h at 4 °C twice. Polymer-  
459 modified liposomes were also prepared according to the above procedure using dry  
460 membrane of a lipid mixture with polymers (lipids/polymer = 7/3, w/w). For  
461 encapsulation of DOX, dry membrane of a lipid mixture with polymers was dispersed in  
462 300 mM ammonium sulfate (pH 6.0). The obtained liposome suspension was extruded  
463 through a polycarbonate membrane with a pore diameter of 100 nm and outer phase of  
464 liposome was substituted to PBS (pH 7.4) for formation of pH gradient. Then aqueous

465 DOX solution (10 mg/mL) was added to the liposome suspension at DOX/lipid (g/mol)  
466 ratio of 75 and the mixed solution was incubated for 1 h at 30 °C. Free DOX was  
467 removed from the liposome suspension by ultracentrifugation for 2 h at 4 °C.  
468 Encapsulation efficiency of DOX by liposomes was estimated from absorbance of DOX  
469 at 499 nm for the DOX-loaded liposomes dissolved in 0.3 M HCl (50%) –ethanol (50%)  
470 before and after purification with ultracentrifugation.

471

472 **Dynamic Light Scattering and Zeta Potential.** Diameters and zeta potentials of the  
473 liposomes (0.2 mM of lipid concentration) were measured using a Zetasizer Nano ZS  
474 ZEN3600 (Malvern Instruments Ltd, Worcestershire, UK). Data was obtained as an  
475 average of more than three measurements on different samples.

476

477 **Release of Pyranine from Liposome.** Release of pyranine from liposome was  
478 measured as previously reported.<sup>29-33,44</sup> To a suspension of pyranine-loaded EYPC  
479 liposomes (lipid concentration  $2.0 \times 10^{-5}$  M) in PBS of varying pHs was added varying  
480 HA derivatives dissolved in the same buffer. For evaluation of polymer-modified  
481 liposomes, pyranine-loaded liposomes (lipid concentration:  $2.0 \times 10^{-5}$  M) were added  
482 to PBS of varying pH at 37 °C and fluorescence intensity (512 nm) of the mixed

483 suspension was followed with excitation at 416 nm using a spectrofluorometer (Jasco  
484 FP-6500, FP-6200). The percent release of pyranine from liposomes was defined as  
485  $\text{Release (\%)} = (F_t - F_i) / (F_f - F_i) \times 100$   
486 where  $F_i$  and  $F_t$  mean the initial and intermediary fluorescence intensities of the  
487 liposome suspension, respectively.  $F_f$  is the fluorescent intensity of the liposome  
488 suspension after the addition of TritonX-100 (final concentration: 0.1%).

489

490 **Immunostaining of CD44 on cells.** Cells ( $2 \times 10^5$  cells) cultured for overnight in 35-  
491 mm glass-bottom dishes were washed with PBS, and then incubated in phenol red-free  
492 DMEM containing 10% FBS and 1% BSA (1 mL). PE-labeled anti-human CD44  
493 antibody (10  $\mu\text{L}$ , BD Biosciences) was added gently to the cells and incubated for 4 h at  
494 37 °C. After the incubation, the cells were washed with PBS three times. Confocal laser  
495 scanning microscopic (CLSM) analysis of these cells was performed using LSM 5  
496 EXCITER (Carl Zeiss Co. Ltd.). For flow cytometric analysis, cells ( $1 \times 10^6$  cells) were  
497 suspended in PBS containing 2% FBS (100  $\mu\text{L}$ ). Subsequently, PE-labeled anti-human  
498 CD44 antibody (10  $\mu\text{L}$ , BD Biosciences) or anti-mouse CD44 antibody (0.2  $\mu\text{g}/\mu\text{L}$ , 1  
499  $\mu\text{L}$ , BD Biosciences) was added gently to the cells and incubated for 30 min at 4 °C in  
500 the dark. The cells were washed with PBS containing 0.1% BSA three times.

501 Fluorescence intensity of these cells was determined by a flow cytometric analysis  
502 (CytoFlex, Beckman Coulter, Inc.). Cellular auto fluorescence was subtracted from each  
503 data.

504

505 **Cellular Association of Liposomes and Inhibition Assay.** Liposomes containing DiI  
506 were prepared as described above except that a mixture of polymer and lipid containing  
507 DiI (0.1 mol%) was dispersed in PBS. Cells ( $5 \times 10^4$  cells) cultured for overnight in 24-  
508 well plates were washed with PBS, and then incubated in serum-free DMEM (0.25 mL).  
509 The DiI-labeled liposomes (0.5 mM lipid concentration, 0.25 mL) were added gently to  
510 the cells and incubated for 4 h at 37 °C. After the incubation, the cells were washed with  
511 PBS three times. Fluorescence intensity of these cells was determined by a flow  
512 cytometric analysis (CytoFlex, Beckman Coulter, Inc.). Cellular auto fluorescence for  
513 each cell was subtracted from each data. DiI fluorescence of each liposome was  
514 measured and cellular fluorescence shown in Figure 7 was corrected using liposomal  
515 fluorescence intensity. For inhibition assay, free HA (10 mg/mL), CHex-HA (1 mg/mL)  
516 and CHex-Dex (1 mg/mL) were pre-incubated to cells for an hour before the incubation  
517 of DiI-labeled liposomes for 4 h.

518

519 **Intracellular Behavior of Liposomes.** Cells ( $2 \times 10^5$  cells) cultured for overnight in  
520 35-mm glass-bottom dishes were washed with PBS, and then incubated in serum-free  
521 DMEM (1 mL). The DiI-labeled liposomes (1 mM lipid concentration, 1 mL) or DOX-  
522 loaded liposomes (4  $\mu\text{g}/\text{mL}$  DOX concentration, 1 mL) were added gently to the cells  
523 and incubated for 4 h at 37 °C. After the incubation, the cells were washed with PBS  
524 three times. CLSM analysis of these cells was performed using LSM 5 EXCITER (Carl  
525 Zeiss Co. Ltd.).

526 **Associated content**

527 **Supporting information**

528 The Supporting Information is available free of charge on the ACS Publications website  
529 at DOI: XXX.

530 Figures and Tables showing the p*K*<sub>a</sub> of HA derivatives, size distribution of  
531 liposomes, CD44 expression in various cells, inhibition assay for colon 26  
532 cells, intracellular distribution of liposomes, characterization of DOX-loaded  
533 liposomes and cytotoxicity of liposomes.

534

535 **Author information**

536 **Corresponding author:**

537 \*E-mail: [yuba@chem.osakafu-u.ac.jp](mailto:yuba@chem.osakafu-u.ac.jp). Phone: +81-722-54-9913. Fax: +81-722-54-  
538 9330.

539

540 **ORCID**

541 Eiji Yuba: 0000-0003-4984-2113

542

543 **Notes**

544 The authors declare no competing financial interest.

545

546 **Acknowledgments**

547 This work was supported by JSPS KAKENHI Grant number (15H03024) and  
548 the Kao Foundation for Arts and Sciences.

549

550 **Abbreviations**

551 HA, hyaluronic acid; DOX, doxorubicin; MGlu, 3-methyl glutarylated; CHex, 2-  
552 carboxycyclohexane-1-carboxylated; EYPC, egg yolk phosphatidylcholine; Dex,  
553 dextran; CLSM, confocal laser scanning microscopy

554

555 **References**

- 556 1. Duncan, R. (2003) The dawning era of polymer therapeutics. *Nat. Rev. Drug Discov.*  
557 2, 347–360.
- 558 2. Mura, S., Nicolas, J., Couvreur, P. (2013) Stimuli-responsive nanocarriers for drug  
559 delivery. *Nat. Mater.* 12, 991–1003.
- 560 3. Stewart, M. P., Sharei, A., Ding, X., Sahay, G., Langer, R., Jensen, K. F. (2016) In  
561 vitro and ex vivo strategies for intracellular delivery. *Nature* 538, 183–192.
- 562 4. Maeda, H., Wu, J., Sawa, T., Matsumura, Y., Hori, K. (2000) Tumor vascular  
563 permeability and the EPR effect in macromolecular therapeutics: a review. *J.*  
564 *Control. Release* 65, 271–284.
- 565 5. Cabral, H., Matsumoto, Y., Mizuno, K., Chen, Q., Murakami, M., Kimura, M.,  
566 Terada, Y., Kano, M. R., Miyazono, K., Uesaka, M., et al. (2011) Accumulation of  
567 sub-100 nm polymeric micelles in poorly permeable tumours depends on size. *Nat.*  
568 *Nanotechnol.* 6, 815–823.
- 569 6. Barenholz, Y. (2012) Doxil® – the first FDA-approved nano-drug: lessons learned.  
570 *J. Control. Release* 160, 117–134.
- 571 7. Iyer, A. K., Singh, A., Ganta, S., Amiji, M. M. (2013) Role of integrated cancer  
572 nanomedicine in overcoming drug resistance. *Adv. Drug Deliv. Rev.* 65, 1784–1802.

- 573 8. Temming, K., Schiffelers, R. M., Molema, G., Kok, R. J. (2005) RGD-based  
574 strategies for selective delivery of therapeutics and imaging agents to the tumour  
575 vasculature. *Drug Resist. Updat.* 8, 381–402.
- 576 9. Song, Z., Lin, Y., Zhang, X., Feng, C., Lu, Y., Gao, Y., Dong, C. (2017) Cyclic  
577 RGD peptide-modified liposomal drug delivery system for targeted oral apatinib  
578 administration: enhanced cellular uptake and improved therapeutic effects. *Int. J.*  
579 *Nanomedicine* 12, 1941–1958.
- 580 10. Sriraman, S. K., Salzano, G., Sarisozen, C., Torchilin, V. (2016) Anti-cancer  
581 activity of doxorubicin-loaded liposomes co-modified with transferrin and folic  
582 acid. *Eur. J. Pharm. Biopharm.* 105, 40–49.
- 583 11. Kono, K., Takashima, M., Yuba, E., Harada, A., Hiramatsu, Y., Kitagawa, H., Otani,  
584 T., Maruyama, K., Aoshima, S. (2015) Multifunctional liposomes having target  
585 specificity, temperature-triggered release, and near-infrared fluorescence imaging  
586 for tumor-specific chemotherapy. *J. Control. Release* 216, 69–77.
- 587 12. Wang, M., Li, J., Li, X., Mu, H., Zhang, X., Shi, Y., Chu, Y., Wang, A., Wu, Z.,  
588 Sun, K. (2016) Magnetically and pH dual responsive dendrosomes for tumor  
589 accumulation enhanced folate-targeted hybrid drug delivery. *J. Control. Release.*  
590 232, 161–174.

- 591 13. Kono, K., Ozawa, T., Yoshida, T., Ozaki, F., Ishizaka, Y., Maruyama, K., Kojima, C.,  
592 Harada, A., Aoshima, S. (2010) Highly temperature-sensitive liposomes based on a  
593 thermosensitive block copolymer for tumor-specific chemotherapy. *Biomaterials* 31,  
594 7096–7105.
- 595 14. Guo, Y., Zhang, Y., Ma, J., Li, Q., Li, Y., Zhou, X., Zhao, D., Song, H., Chen, Q.,  
596 Zhu, X. (2017) Light/magnetic hyperthermia triggered drug released from multi-  
597 functional thermo-sensitive magnetoliposomes for precise cancer synergetic  
598 theranostics. *J. Control. Release* in press.
- 599 15. Matsuki, D., Adewale, O., Horie, S., Okajima, J., Komiya, A., Oluwafemi, O.,  
600 Maruyama, S., Mori, S., Kodama, T. (2017) Treatment of tumor in lymph nodes  
601 using near-infrared laser light-activated thermosensitive liposome-encapsulated  
602 doxorubicin and gold nanorods. *J. Biophotonics* in press.
- 603 16. Yan, F., Duan, W., Li, Y., Wu, H., Zhou, Y., Pan, M., Liu, H., Liu, X., Zheng, H.  
604 (2016) NIR-laser-controlled drug release from DOX/IR-780-loaded temperature-  
605 sensitive-liposomes for chemo-photothermal synergistic tumor therapy.  
606 *Theranostics* 6, 2337–2351.

- 607 17. Li, T., Amari, T., Semba, K., Yamamoto, T., Takeoka, S. (2017) Construction and  
608 evaluation of pH-sensitive immunoliposomes for enhanced delivery of anticancer  
609 drug to ErbB2 over-expressing breast cancer cells. *Nanomedicine 13*, 1219–1227.
- 610 18. Vila-Caballer, M., Codolo, G., Munari, F., Malfanti, A., Fassan, M., Rugge, M.,  
611 Balasso, A., de Bernard, M., Salmaso, S. (2016) A pH-sensitive stearyl-PEG-  
612 poly(methacryloyl sulfadimethoxine)-decorated liposome system for protein  
613 delivery: An application for bladder cancer treatment. *J. Control. Release 238*, 31–  
614 42.
- 615 19. Zhao, Y., Ren, W., Zhong, T., Zhang, S., Huang, D., Guo, Y., Yao, X., Wang, C.,  
616 Zhang, W. Q., Zhang, X., et al. (2016) Tumor-specific pH-responsive peptide-  
617 modified pH-sensitive liposomes containing doxorubicin for enhancing glioma  
618 targeting and anti-tumor activity. *J. Control. Release 222*, 56–66.
- 619 20. Dai, M., Wu, C., Fang, H. M., Li, L., Yan, J. B., Zeng, D. L., Zou, T. (2017)  
620 Thermo-responsive magnetic liposomes for hyperthermia-triggered local drug  
621 delivery. *J. Microencapsul. 34*, 408–415.
- 622 21. Luo, L., Bian, Y., Liu, Y., Zhang, X., Wang, M., Xing, S., Li, L., Gao, D. (2016)  
623 Gold nanoshells: combined near infrared photothermal therapy and chemotherapy  
624 using gold nanoshells coated liposomes to enhance antitumor effect. *Small 12*, 4102.

- 625 22. Swenson, C. E., Haemmerich, D., Maul, D. H., Knox, B., Ehrhart, N., Reed, R. A.  
626 (2015) Increased duration of heating boosts local drug deposition during  
627 radiofrequency ablation in combination with thermally sensitive liposomes  
628 (ThermoDox) in a porcine model. *PLoS One* 10, e0139752.
- 629 23. Mikhail, A. S., Negussie, A. H., Pritchard, W. F., Haemmerich, D., Woods, D.,  
630 Bakhutashvili, I., Esparza-Trujillo, J., Brancato, S. J., Karanian, J., Agarwal, P. K.,  
631 et al. (2017) Lyso-thermosensitive liposomal doxorubicin for treatment of bladder  
632 cancer. *Int. J. Hyperthermia* 1–8.
- 633 24. Dou, Y., Hynynen, K., Allen, C. (2017) To heat or not to heat: Challenges with  
634 clinical translation of thermosensitive liposomes. *J. Control. Release* 249, 63–73.
- 635 25. Ellens, H., Bentz, J., Szoka, F. C. (1984) pH-Induced destabilization of  
636 phosphatidylethanolamine-containing liposomes: role of bilayer contact.  
637 *Biochemistry* 23, 1532–1538.
- 638 26. Seki, K., Tirrell, D. A. (1984) pH-Dependent complexation of poly(acrylic acid)  
639 derivatives with phospholipid vesicle membrane. *Macromolecules* 17, 1692–1698.
- 640 27. Murthy, N., Robichaud, J. R., Tirrell, D. A., Stayton, P. S., Hoffman, A. S. (1999)  
641 The design and synthesis of polymers for eukaryotic membrane disruption. *J.*  
642 *Control. Release* 61, 137–143.

- 643 28. Kono, K., Igawa, T., Takagishi, T. (1997) Cytoplasmic delivery of calcein mediated  
644 by liposomes modified with a pH-sensitive poly(ethylene glycol) derivative.  
645 *Biochim. Biophys. Acta* 1325, 143–154.
- 646 29. Sakaguchi, N., Kojima, C., Harada, A., Kono, K. (2008) Preparation of pH-sensitive  
647 poly(glycidol) derivatives with varying hydrophobicities: their ability to sensitize  
648 stable liposomes to pH. *Bioconjug. Chem.* 19, 1040–1048.
- 649 30. Yuba, E., Harada, A., Sakanishi, Y., Kono, K. (2011) Carboxylated hyperbranched  
650 poly(glycidol)s for preparation of pH-sensitive liposomes. *J. Control. Release*, 149,  
651 72-80.
- 652 31. Yuba, E., Tajima, N., Yoshizaki, Y., Harada, A., Hayashi, H., Kono, K. (2014)  
653 Dextran derivative-based pH-sensitive liposomes for cancer immunotherapy.  
654 *Biomaterials* 35, 3091–3101.
- 655 32. Yuba, E., Yamaguchi, A., Yoshizaki, Y., Harada, A., Kono, K. (2017) Bioactive  
656 polysaccharide-based pH-sensitive polymers for cytoplasmic delivery of antigen and  
657 activation of antigen-specific immunity. *Biomaterials* 120, 32–45.
- 658 33. Yuba, E., Uesugi, S., Miyazaki, M., Kado, Y., Harada, A., Kono, K. (2017)  
659 Development of pH-sensitive dextran derivatives with strong adjuvant function and  
660 their application to antigen delivery. *Membranes* 7, 41.

- 661 34. Cosco, D., Tsapis, N., Nascimento, T. L., Fresta, M., Chapron, D., Taverna, M.,  
662 Arpicco, S., Fattal, E. (2017) Polysaccharide-coated liposomes by post-insertion of a  
663 hyaluronan-lipid conjugate. *Colloids Surf. B Biointerfaces* 158, 119–126.
- 664 35. Mattheolabakis, G., Milane, L., Singh, A., Amiji, M. M. (2015) Hyaluronic acid  
665 targeting of CD44 for cancer therapy: from receptor biology to nanomedicine. *J.*  
666 *Drug Target.* 23, 605–618.
- 667 36. Zhang, Y., Chan, J. W., Moretti, A., Uhrich, K. E. (2015) Designing polymers with  
668 sugar-based advantages for bioactive delivery applications. *J. Control. Release* 219,  
669 355–368.
- 670 37. Kang, B., Opatz, T., Landfester, K., Wurm, F. R. (2015) Carbohydrate nanocarriers  
671 in biomedical applications: functionalization and construction. *Chem. Soc. Rev.* 44,  
672 8301–8325.
- 673 38. Miyazaki, M., Yuba, E., Harada, A., Kono, K. (2015) Hyaluronic acid derivative-  
674 modified liposomes as pH-sensitive anticancer drug delivery system. *J. Control.*  
675 *Release* 213, e73–e74.
- 676 39. Weissmann, B., Meyer, K. (1954) The structure of hyalobiuronic acid and of  
677 hyaluronic acid from umbilical cord. *J. Am. Chem. Soc.* 27, 1753–1757.
- 678 40. Platt, V. M., Szoka, F. C. Jr. (2008) Anticancer therapeutics: targeting

679 macromolecules and nanocarriers to hyaluronan or CD44, a hyaluronan receptor.  
680 *Mol. Pharm.* 5, 474–486.

681 41. Hyukijin, L., Kyuri, L., Tae, G. P. (2008) Hyaluronic acid–paclitaxel conjugate  
682 micelles: synthesis, characterization, and antitumor activity. *Bioconjug. Chem.* 19,  
683 1319–1325.

684 42. Magnani, A., Silvestri, V., Barbucci, R. (1999) Hyaluronic acid and sulfated  
685 hyaluronic acid in aqueous solution: effect of the sulfation on the protonation and  
686 complex formation with  $\text{Cu}^{2+}$  and  $\text{Zn}^{2+}$  ions. *Macromol. Chem. Phys.* 200, 2003–  
687 2014.

688 43. Lewrick, F., Süß, R. (2010) Remote loading of anthracyclines into liposomes.  
689 *Methods Mol. Biol.* 605, 139–145.

690 44. Daleke, D. L., Hong, K., Papahadjopoulos, D. (1990) Endocytosis of liposomes by  
691 macrophages: binding, acidification and leakage of liposomes monitored by a new  
692 fluorescence assay. *Biochim. Biophys. Acta* 1024, 352–366.  
693



697 **Supporting information**

698

699 **Hyaluronic acid-based pH-sensitive polymer-modified liposomes for cell-specific**  
700 **intracellular drug delivery systems**

701

702 Maiko Miyazaki<sup>1</sup>, Eiji Yuba<sup>1,\*</sup>, Hiroshi Hayashi<sup>2</sup>, Atsushi Harada<sup>1</sup>, and Kenji Kono<sup>1</sup>

703

704 <sup>1</sup>Department of Applied Chemistry, Graduate School of Engineering, Osaka Prefecture  
705 University, 1-1 Gakuen-cho, Naka-ku, Sakai, Osaka 599-8531, Japan

706 <sup>2</sup>Science Lin, 1-1-35 Nishiawaji, Higashiyodogawa-Ku, Osaka, Osaka 533-0031, Japan

707

708 **\*Corresponding authors: Eiji Yuba**

709 Tel: +81-722-54-9913; Fax: +81-722-54-9330; yuba@chem.osakafu-u.ac.jp

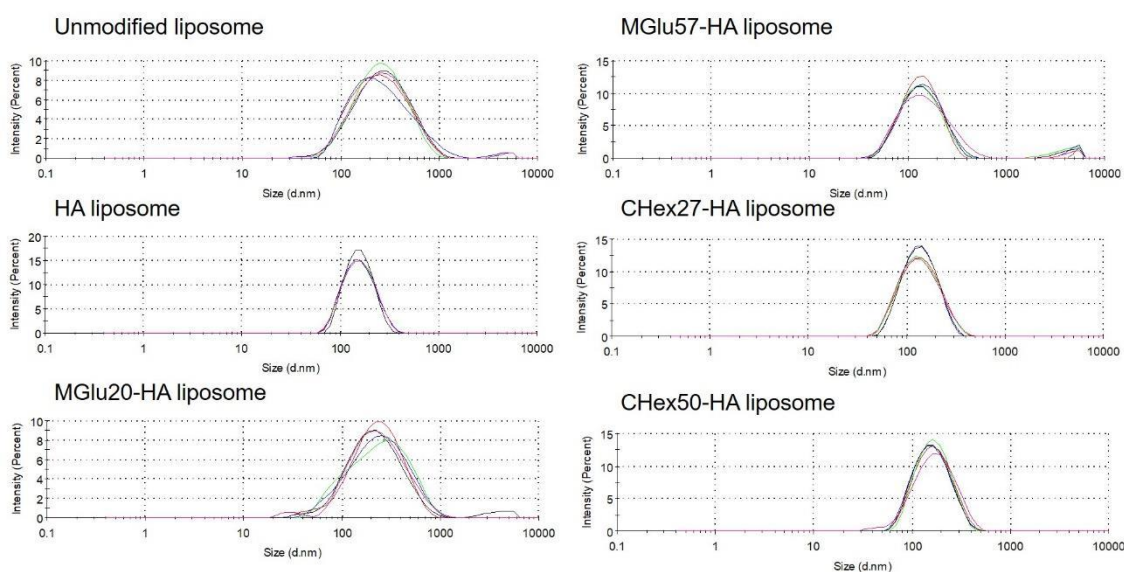
710

711

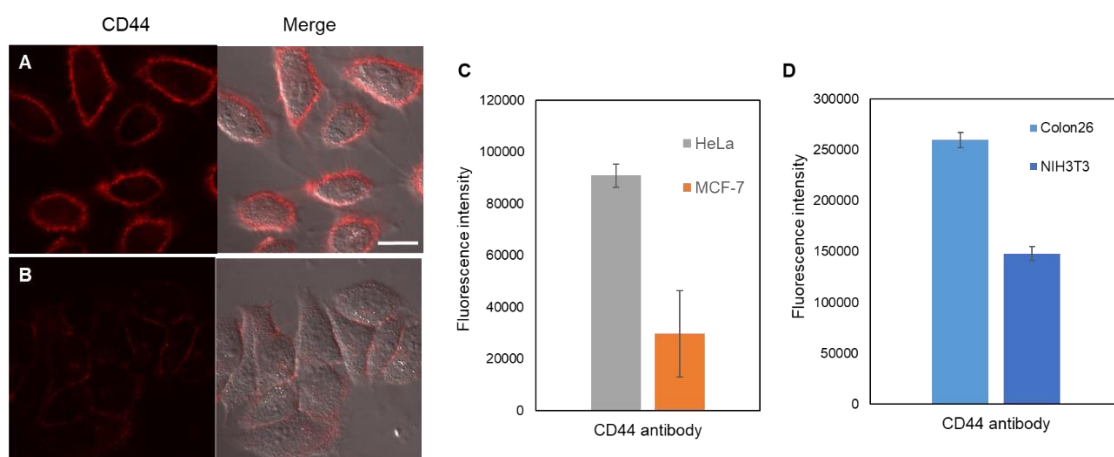
**Table S1. p*K*<sub>a</sub> of HA derivatives**

<b>Polymer</b>	<b>p<i>K</i><sub>a</sub></b>
MGlu10-HA	5.37 ± 0.16
MGlu43-HA	6.01 ± 0.04
MGlu52-HA	6.13 ± 0.02
CHex18-HA	6.33 ± 0.05
CHex34-HA	6.37 ± 0.03
CHex60-HA	6.70 ± 0.01

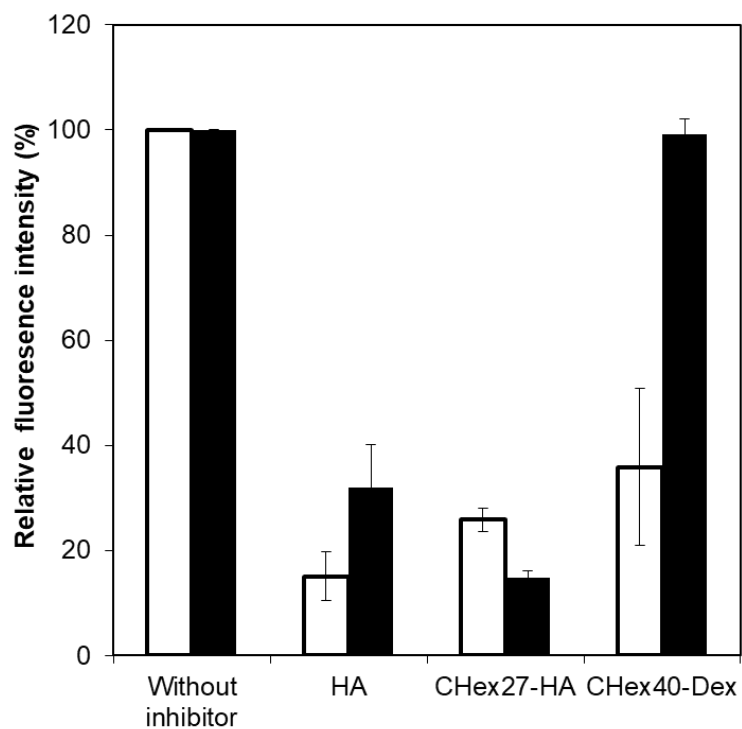
712



713  
 714 **Figure S1.** Size distribution of liposomes modified with or without HA derivatives.  
 715

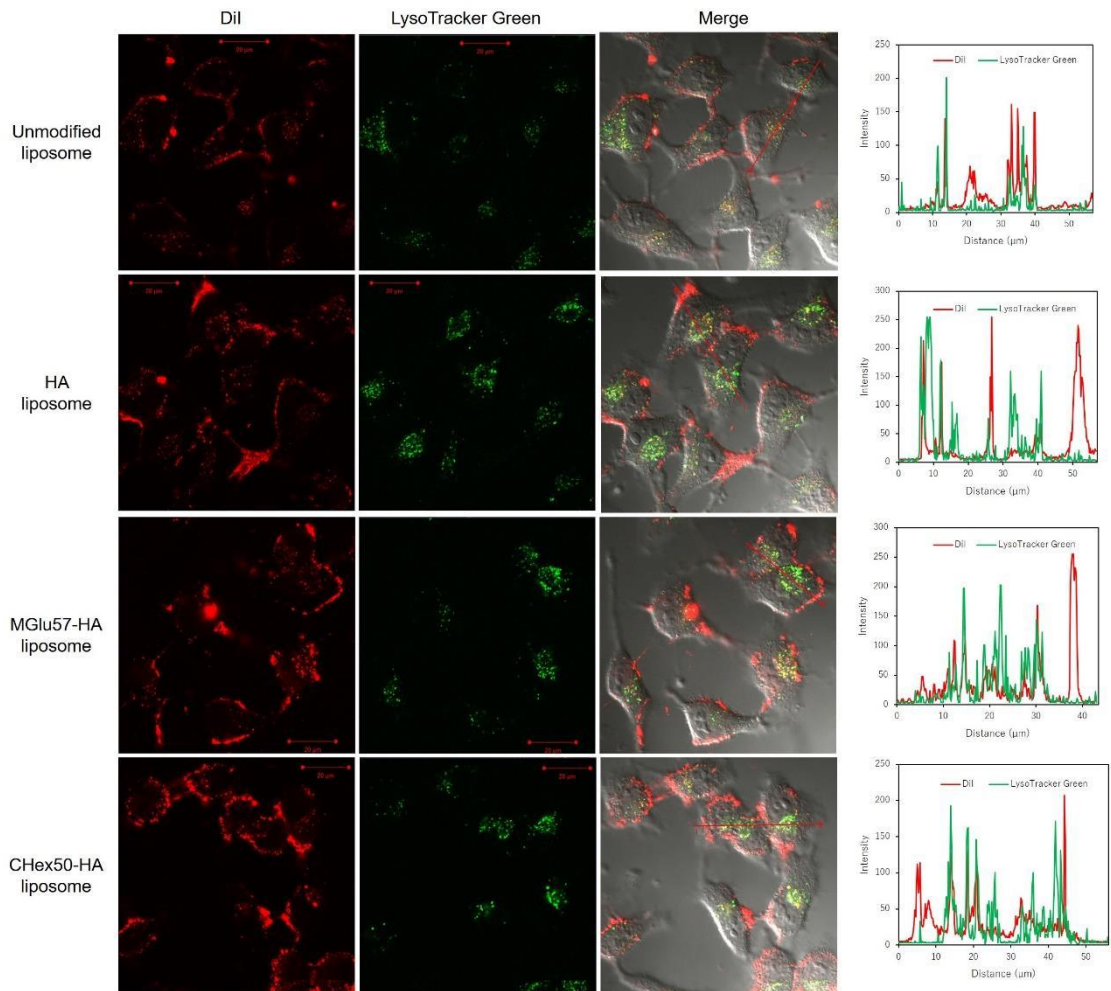


716  
 717 **Figure S2.** Confocal laser scanning microscopic (CLSM) images for HeLa cells (A) or  
 718 MCF-7 (B) cells treated with anti-human PE-CD44 antibody for 4 h at 37 °C in phenol  
 719 red-free 10% FBS medium. Scale bar represents 20  $\mu$ m. (C, D) Fluorescence intensity for  
 720 human cell lines treated with anti-human PE-CD44 antibody (C) or mouse cell treated  
 721 with anti-mouse PE-CD44 antibody (D). Cellular auto fluorescence was corrected.  
 722



723

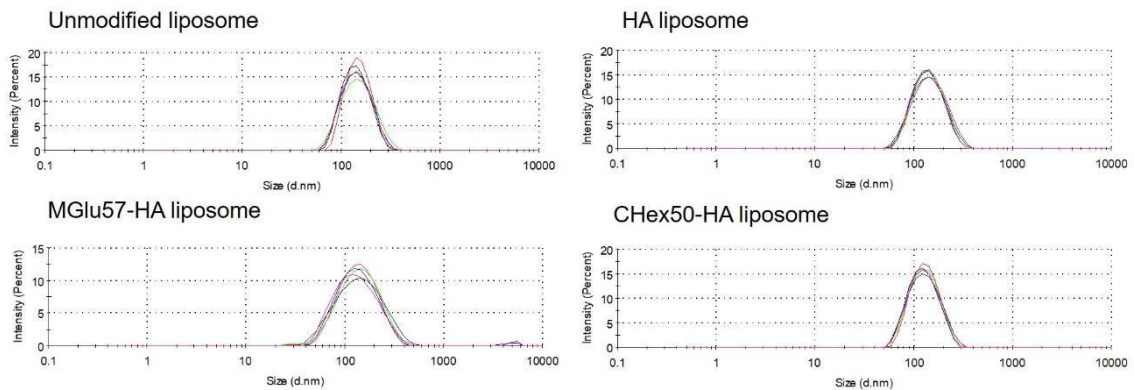
724 **Figure S3.** Inhibition of cellular association of HA-C<sub>10</sub>-modified liposomes (open bars)  
 725 and CHex<sub>27</sub>-HA-C<sub>10</sub>-modified liposomes (closed bars) by various inhibitors. Colon26  
 726 cells were pre-incubated with various inhibitors for 1 h before liposome treatment.  
 727 Relative fluorescence intensity was calculated as the ratios of the amount of association  
 728 in the presence of inhibitor to that in the absence of inhibitor.



729

730 **Figure S4.** CLSM images of HeLa cells treated with DiI-labeled liposomes with or  
 731 without HA derivatives for 4 h. Intracellular acidic organelle was stained by LysoTracker  
 732 Green. Scale bars represent 20  $\mu\text{m}$ . Line profiles of fluorescence intensity in merged  
 733 images were also shown.

734



735

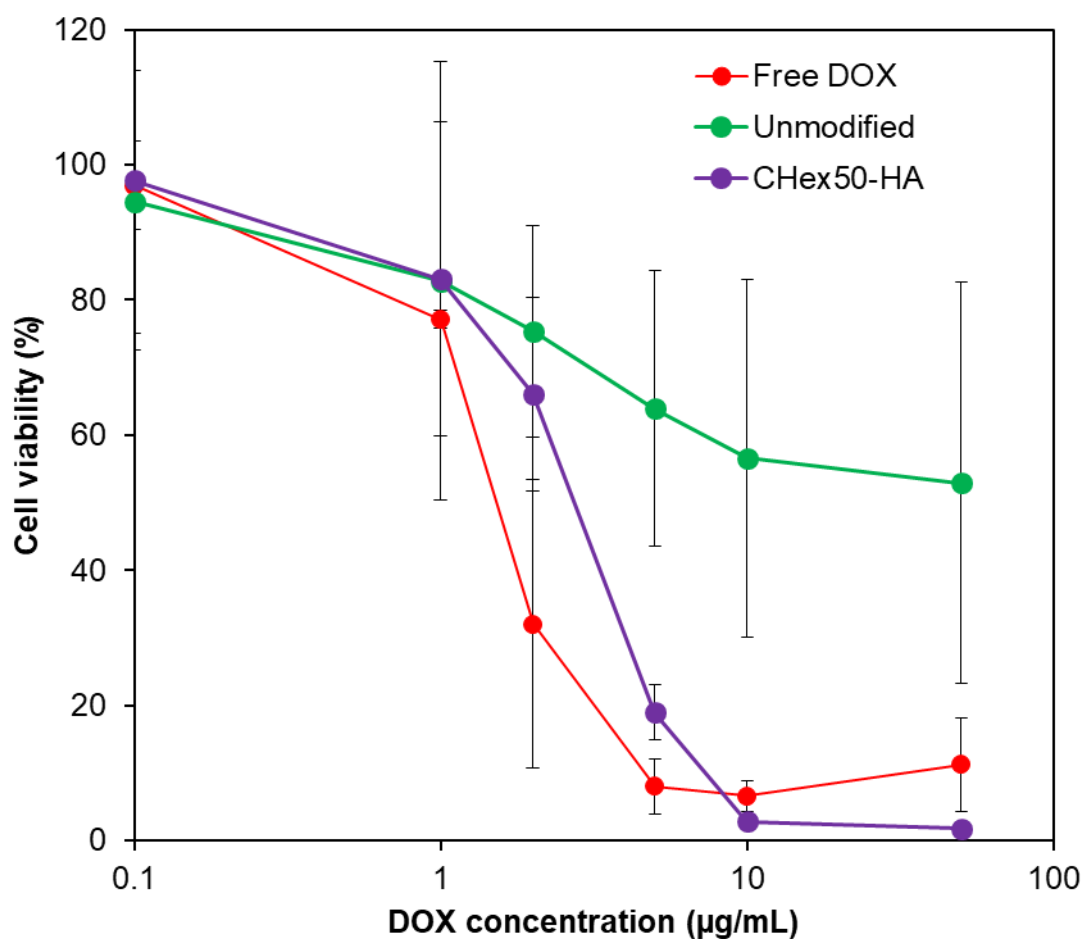
736 **Figure S5.** Size distribution of DOX-liposomes modified with or without HA derivatives.

737

**Table S2. Particle Sizes and Zeta Potentials of DOX-Loaded Liposomes**

Liposome	Encapsulation efficiency (%)	Z-average (nm)	PdI	Zeta potential (mV)
Unmodified	99.7 ± 3.5	138.4 ± 1.2	0.096 ± 0.023	-8.2 ± 0.8
HA-C <sub>10</sub>	97.9 ± 9.6	137.3 ± 2.8	0.103 ± 0.011	-8.8 ± 0.2
MGLu <sub>57</sub> -HA-C <sub>10</sub>	73.3 ± 12.6	122.2 ± 2.0	0.167 ± 0.038	-36.7 ± 1.3
CHex <sub>50</sub> -HA-C <sub>10</sub>	79.5 ± 6.8	131.9 ± 12.2	0.153 ± 0.055	-39.8 ± 0.1

738



739

740 **Figure S6.** Cell viability of HeLa cells treated with free DOX or DOX-loaded liposomes  
 741 modified with or without CHex50-HA as indicating DOX concentrations for 24 h.

742